Development of Wire-Cell Event Reconstruction for LArTPCs in Neutrino Physics

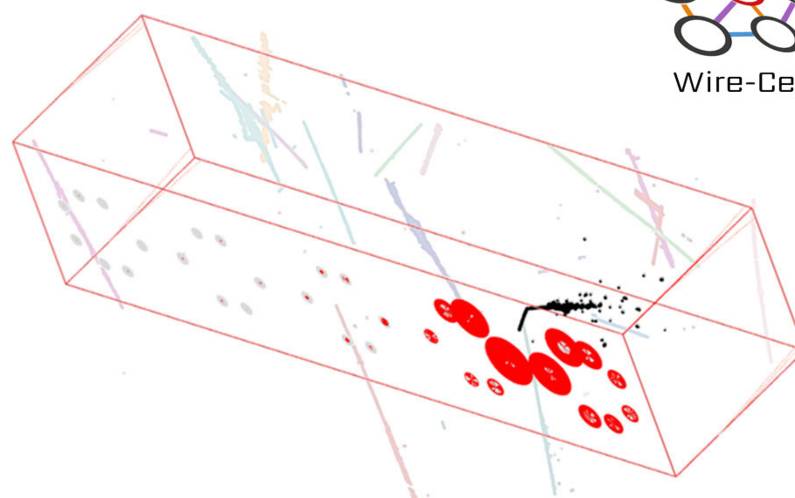

Xin Qian

BNL

Wire-Cell

Fermilab

μBooNE

Brookhaven National Laboratory

Neutrino Oscillation

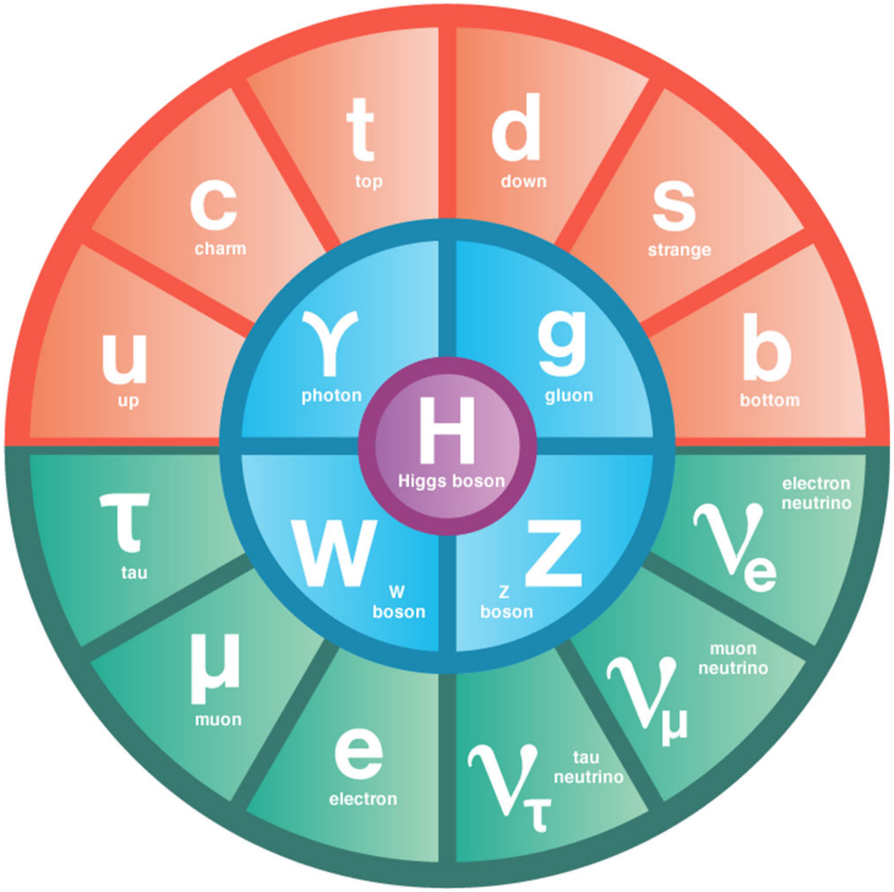

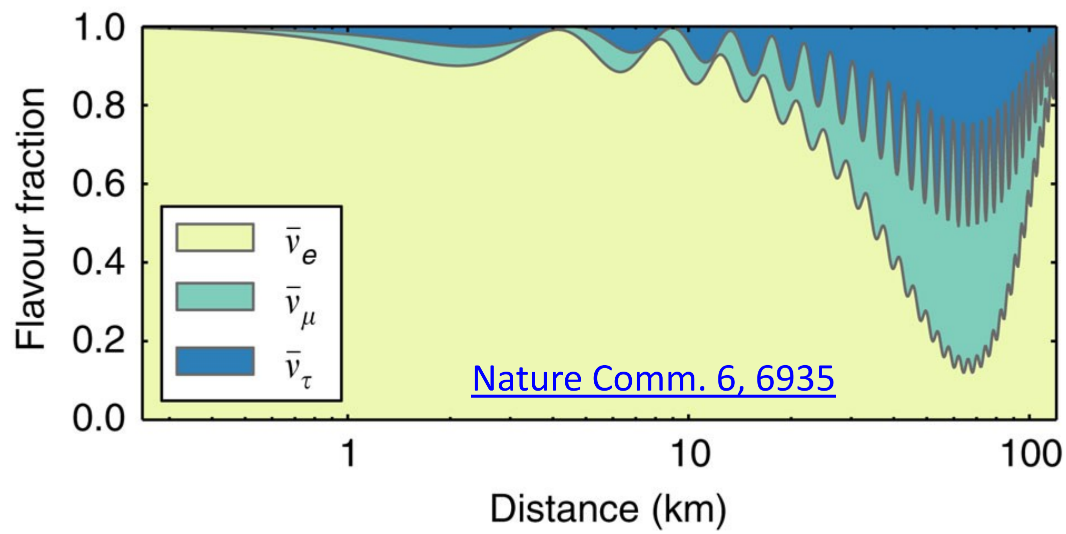

Neutrino oscillation experiments have provided the first evidence for physics beyond the Standard Model of particle physics

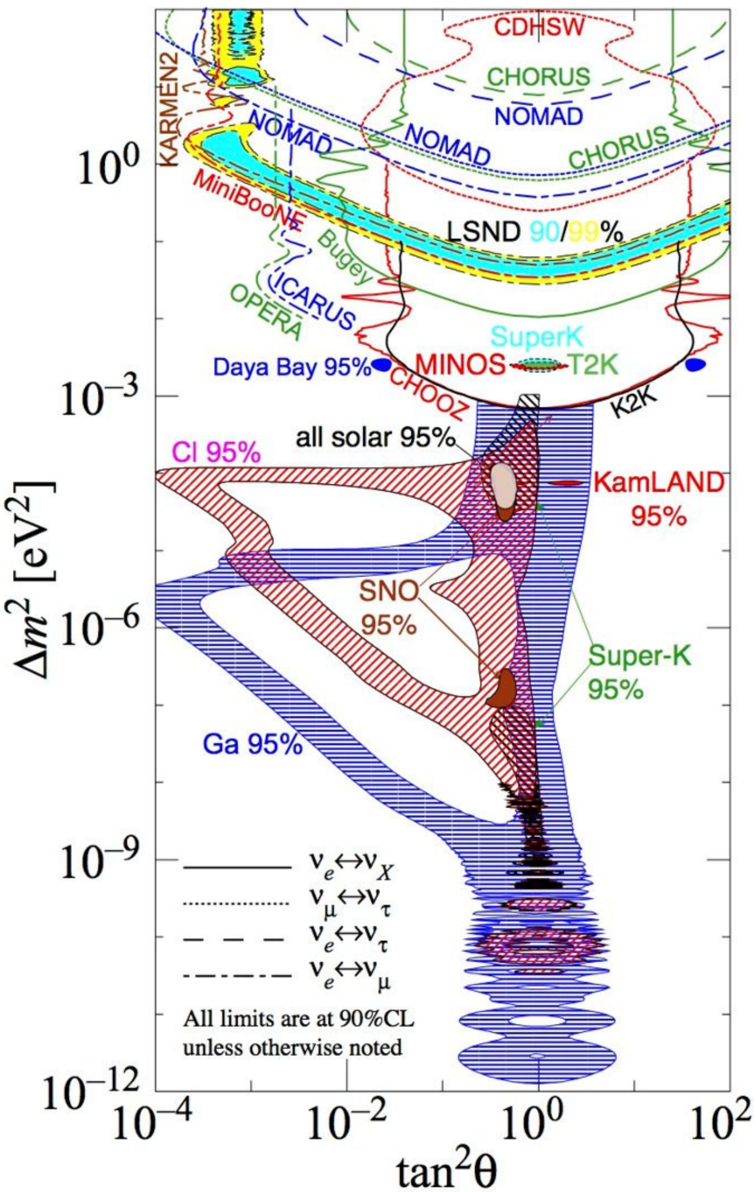

Neutrino Oscillation Experiments

- > 50 years
- > 30 experiments
- > Phase space over tens of orders of magnitude

Courtesy: Hitoshi Murayama

Three-ν Paradigm

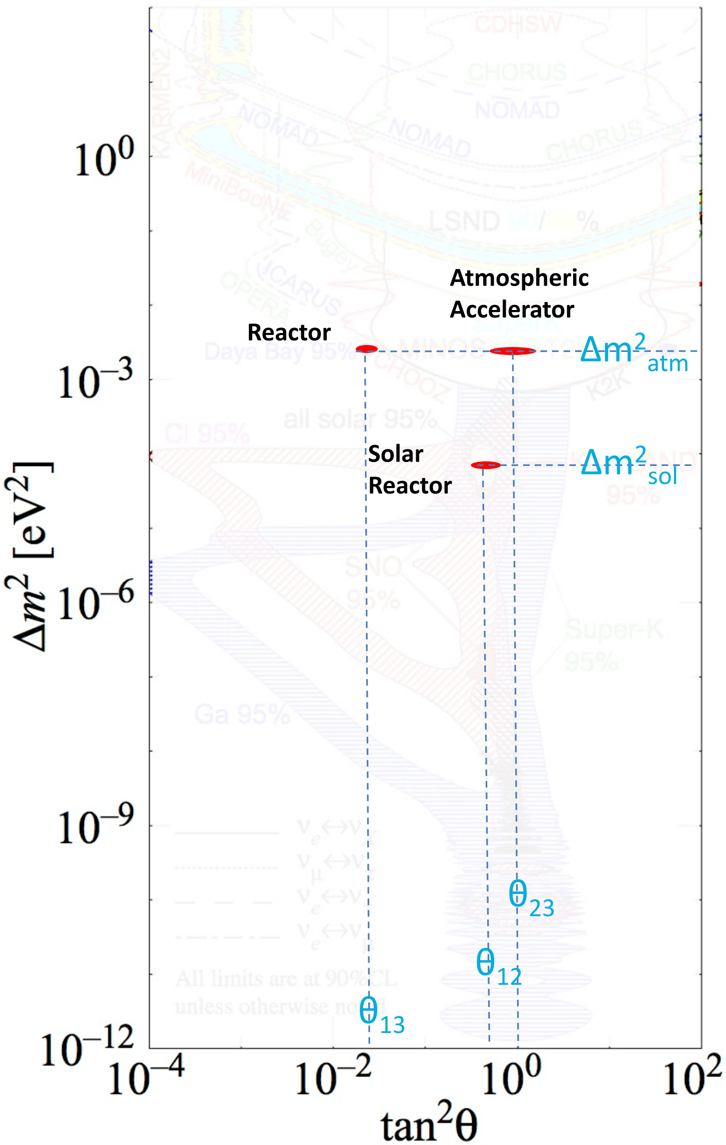

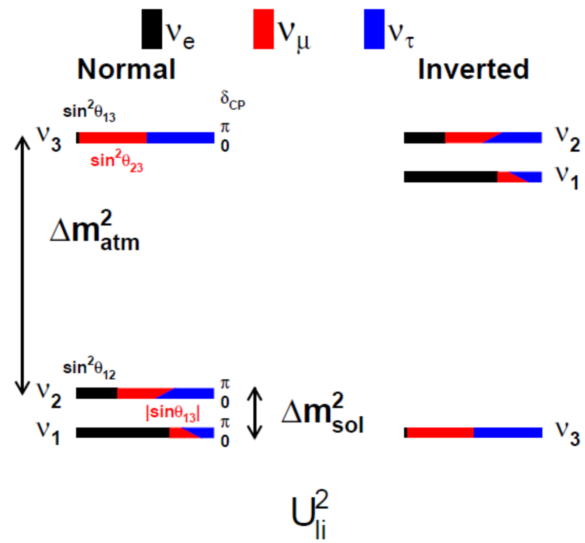

Unknowns: CP phase, normal or inverted mass ordering?

2015 Nobel Prize
Takaaki Kajita &
Arthur B. McDonald

Deep Underground Neutrino Experiment (DUNE)

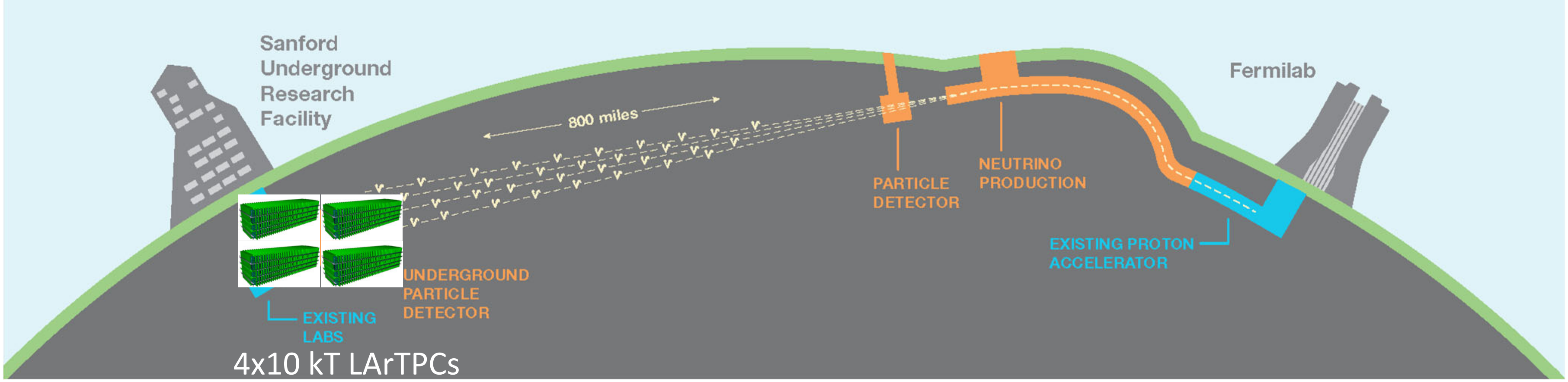

- Search for new CP violation and determine the mass ordering through precision measurement of **(anti)ν_μ→(anti)ν_e oscillation**
  - Also search for proton decay and detection of supernova neutrinos

- Four 10 kT LArTPC detectors (each 20 x 20 x 70 m^3)

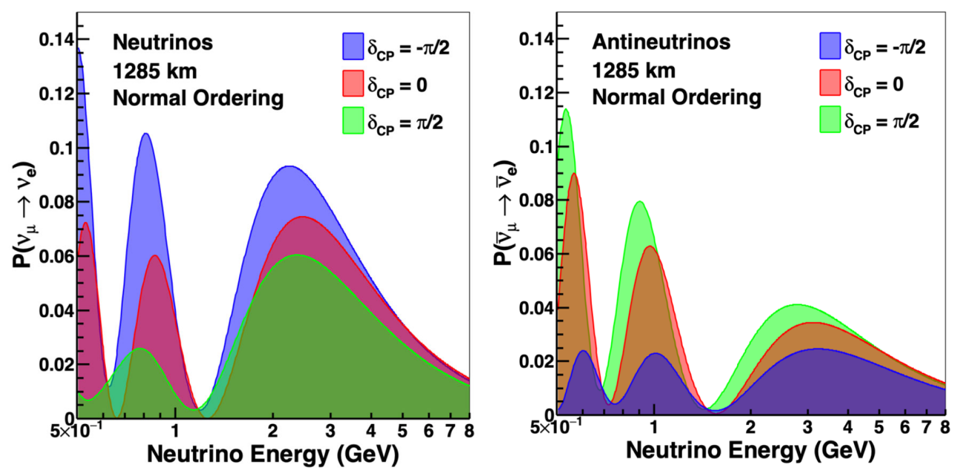

EPJC 80, 978

Experimental Anomalies

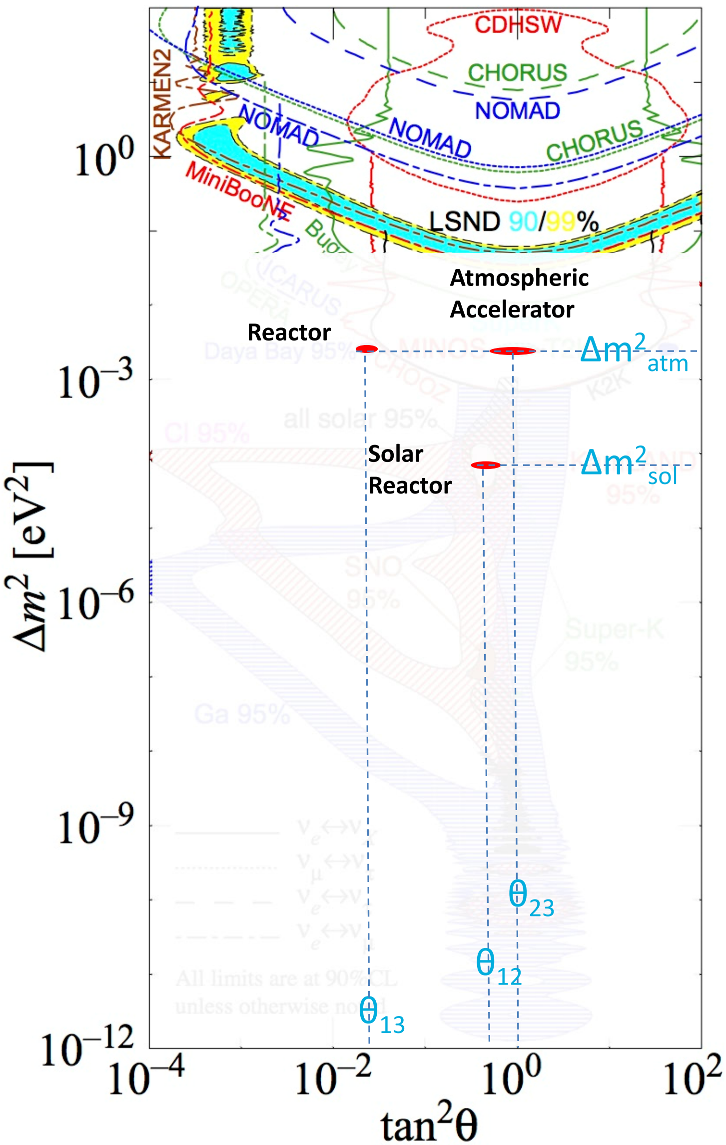

- There are a series of experimental anomalies hinting towards eV scale sterile neutrino(s)
  - Reactor anomaly (missing anti-ν_e?)
  - Gallium anomaly/BEST (missing ν_e?)
  - Neutrino-4 (anti-ν_e oscillation?)
  - LSND and MiniBooNE (anti-ν_e & ν_e appearance?)

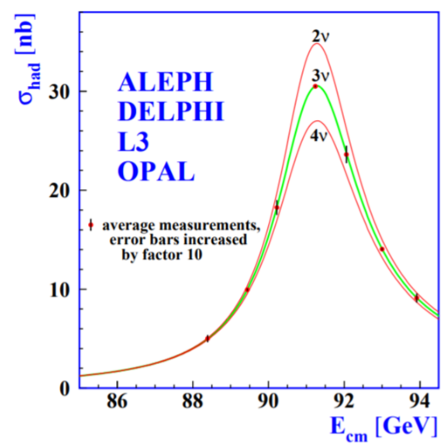

Phys. Rept. 427, 257 (2006)

$N_\nu = 2.9840 \pm 0.0082$

If there are additional neutrinos beyond three, they just don't participate in weak interactions (i.e., "sterile")

Reactor Antineutrino “Anomaly”

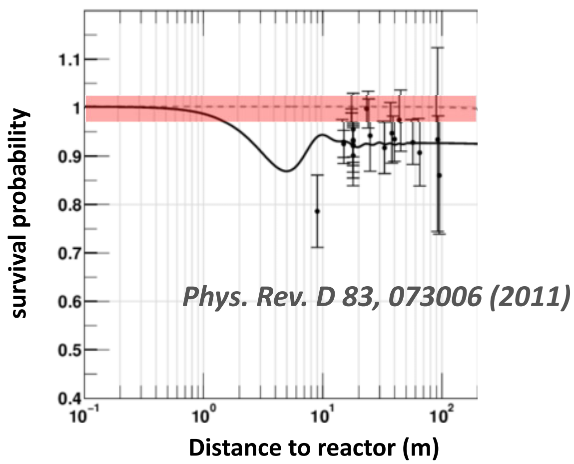

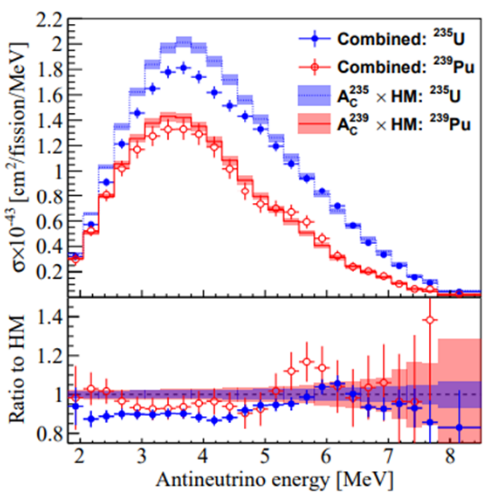

Daya Bay + PROSPECT
arXiv:2106.12251 (2021)

Anomaly in Neutrino Physics

Mistake?

- mistake in experiment?
- mistake in theory?

Discovery?

Solar Neutrino “Anomaly”

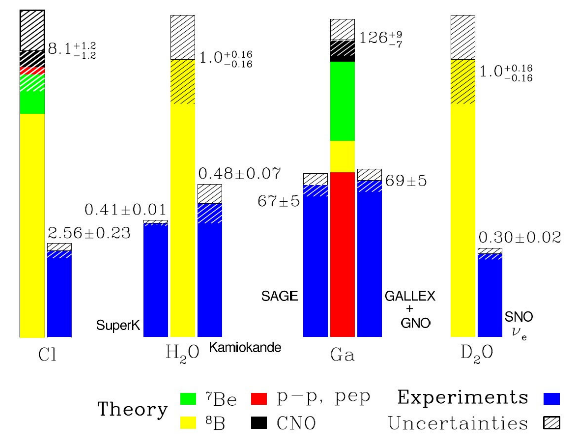

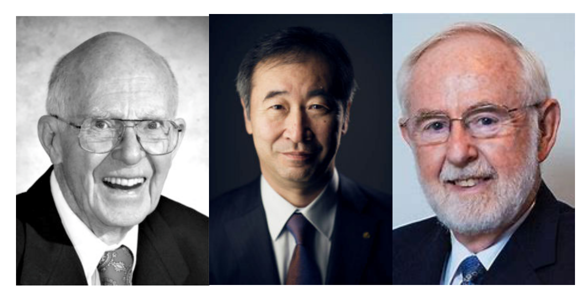

R. Davis **T. Kajita** **A. Mcdonald**

MiniBooNE Anomaly

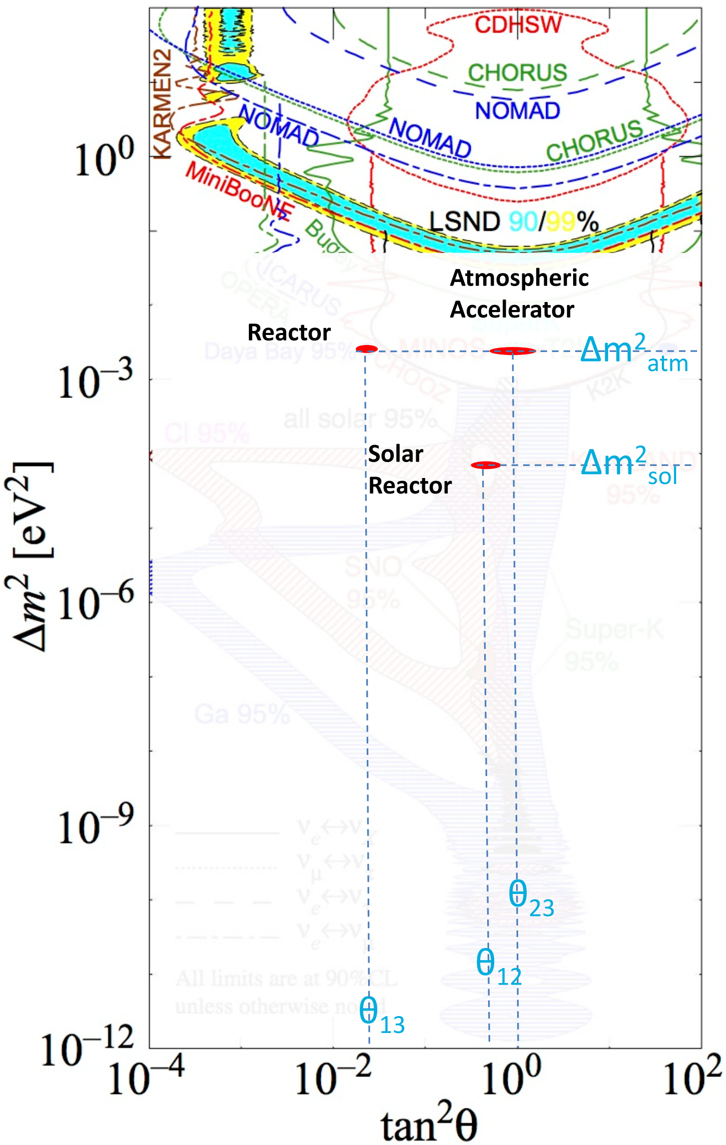

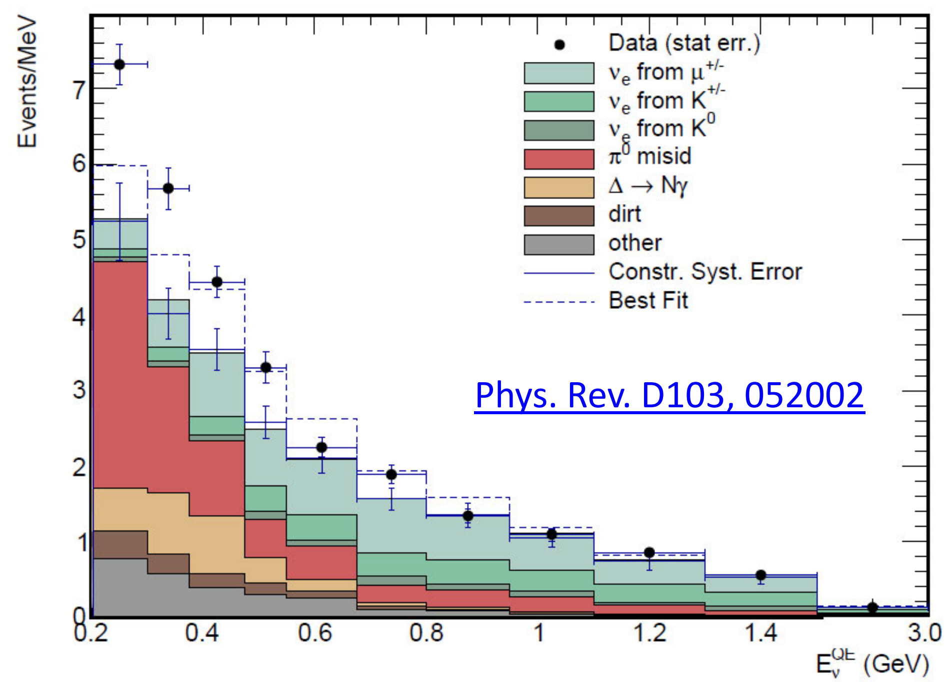

- MiniBooNE (2002-2019) observed low-energy excess (LEE) with 4.8σ (systematics limited) significance
- If LEE is interpreted as ν_e appearance in the primarily ν_μ beam, would suggest 4th (sterile) neutrino

MiniBooNE: A Cherenkov Detector

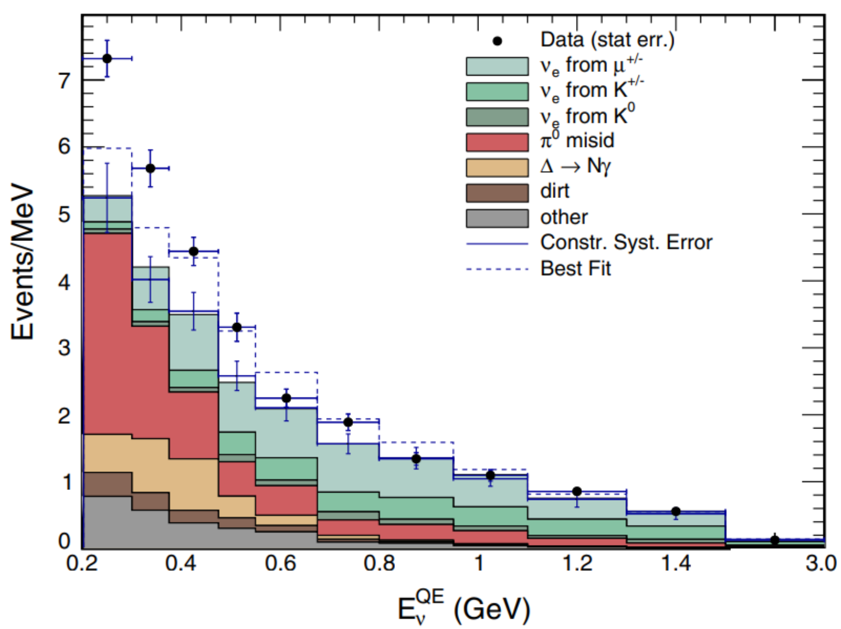

It detected ν_e by the **electrons** produced in charged current (CC) interactions.

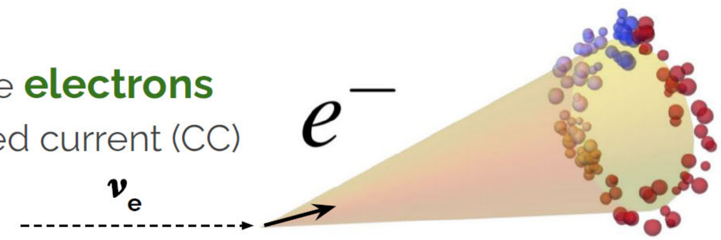

However, **photons**, that pair produce extremely collimated electron/positron pairs produced an identical Cherenkov ring

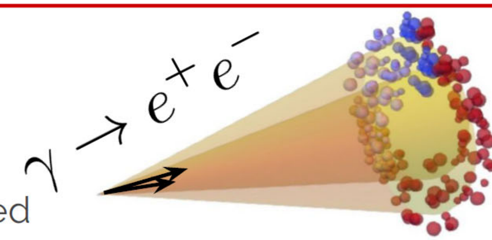

An excellent e/ γ separation can be achieved with the Liquid Argon Time Projection Chamber (LArTPC) technology → MicroBooNE is built to understand the nature of MiniBooNE LEE (e? γ? or what?)

Principle of Single-Phase Liquid Argon Time Projection Chamber (LArTPC)

- ~mm scale position resolution with multiple 1D wire readouts
- Particle identification (PID) with energy depositions and topologies

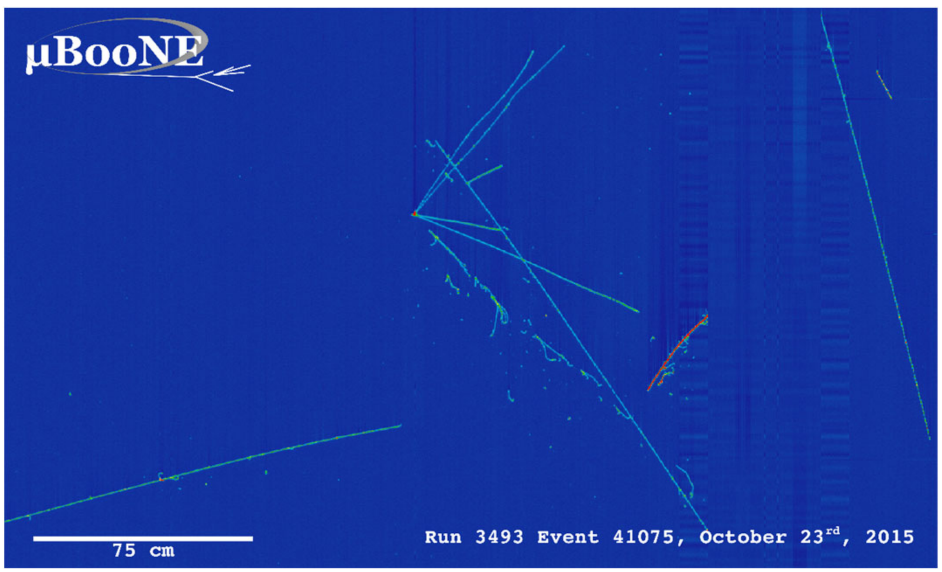

Made by Bo Yu (BNL)

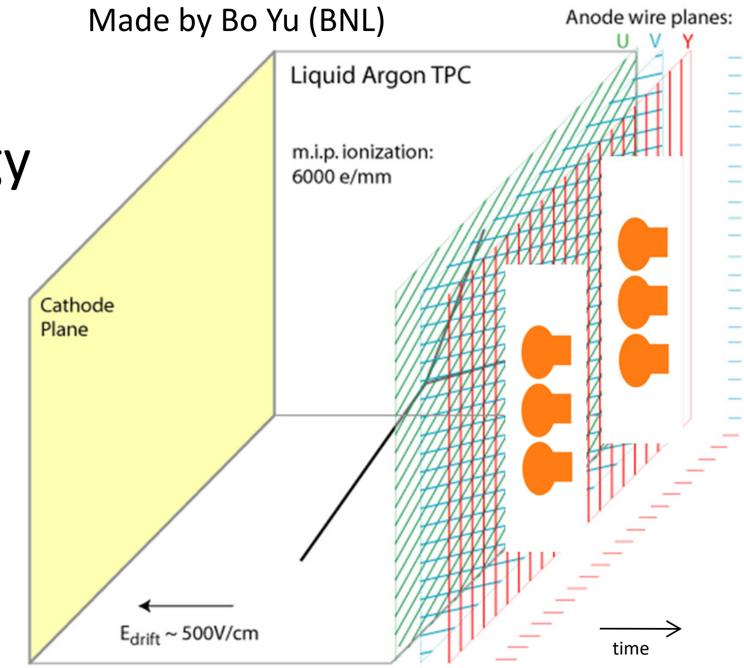

Drift velocity 1.6 km/s → several ms drift time

Separation of e and γ in LArTPC

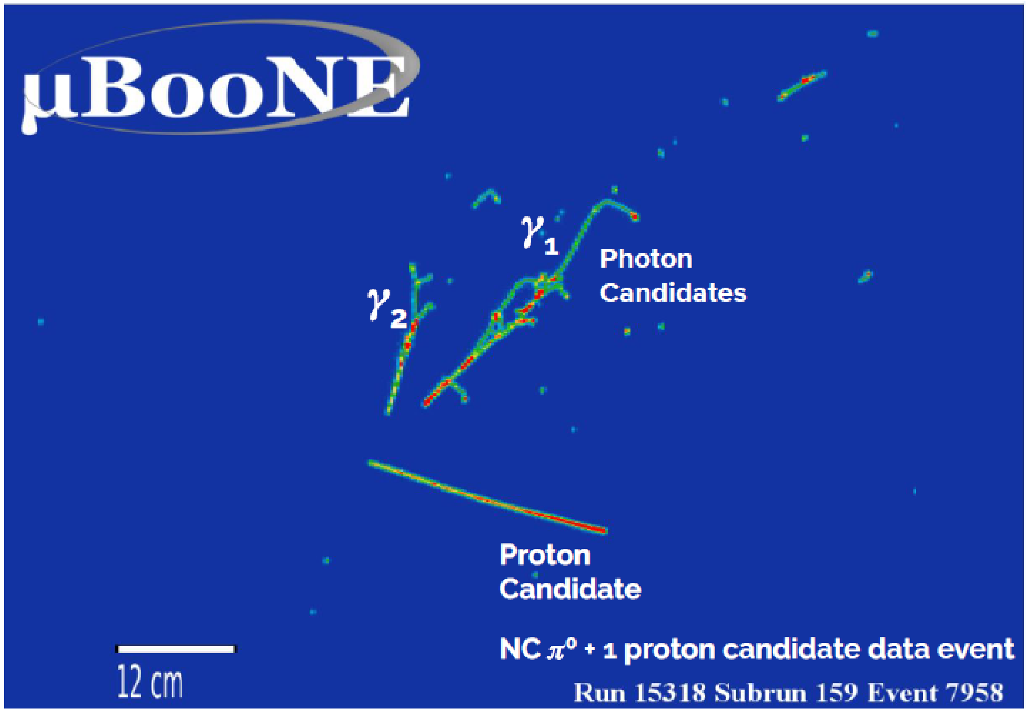

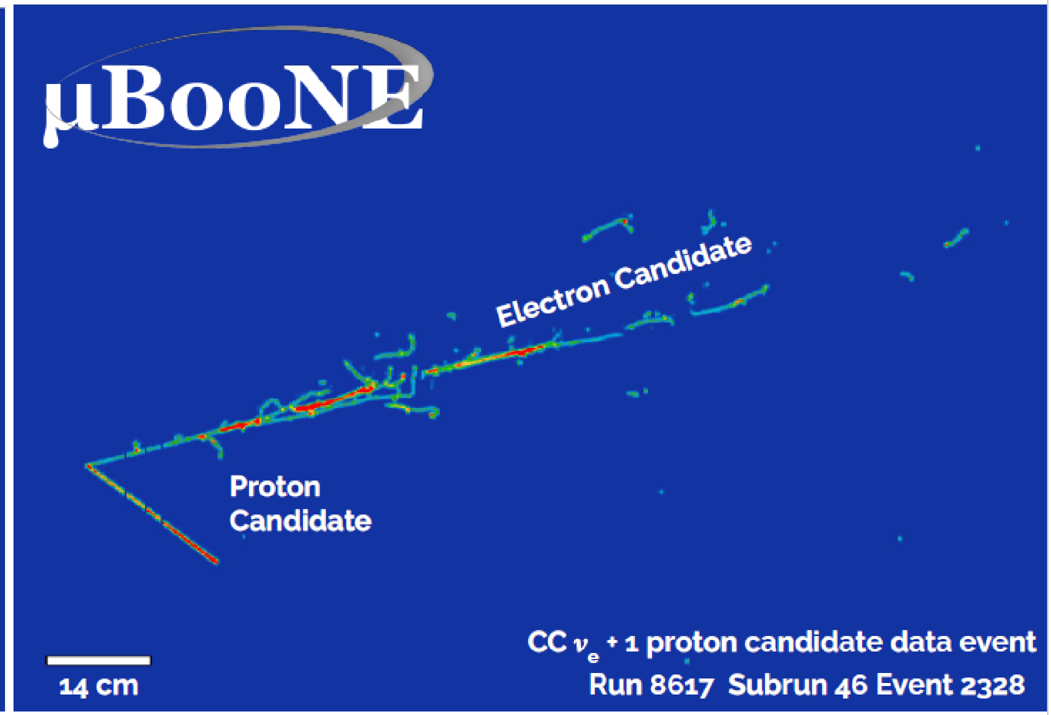

- Event topology to separate EM showers (e/γ) from tracks (proton, muon)

Separation of e and γ in LArTPC

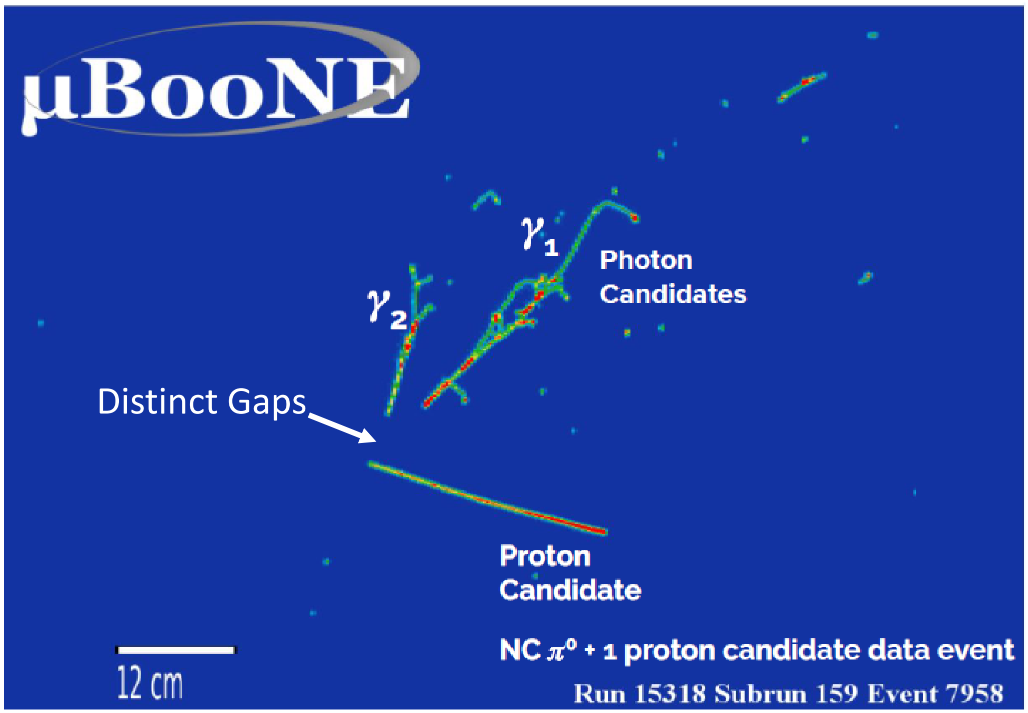

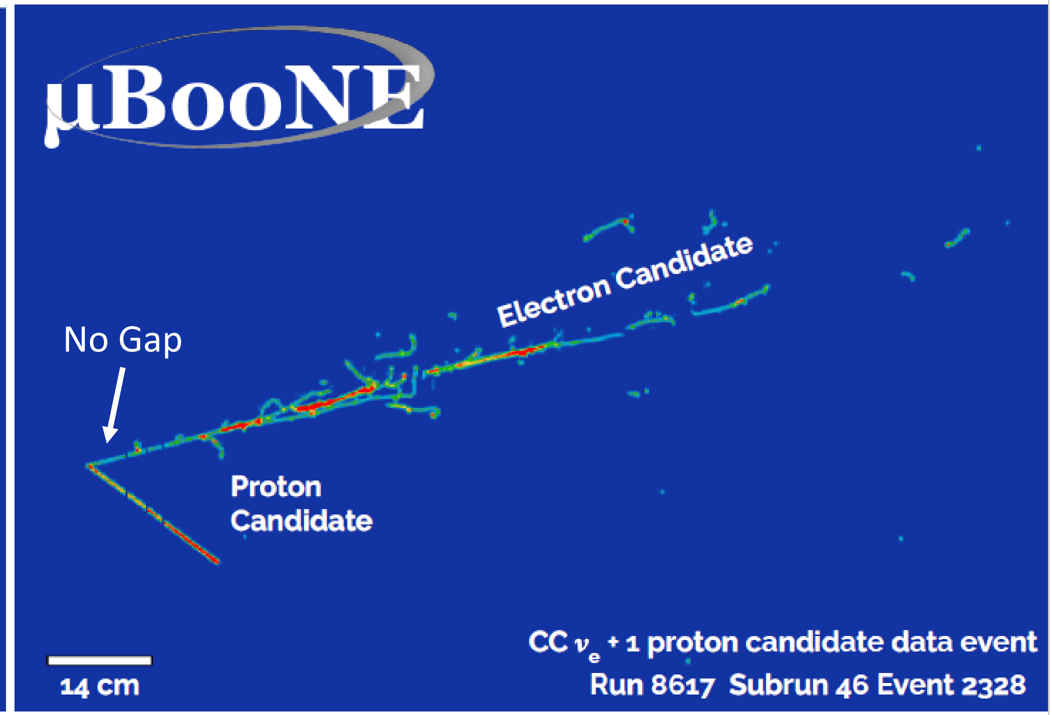

- Event topology to separate EM showers (e/γ) from tracks (proton, muon)
- Separation of e and γ : Gap Identification

Separation of e and γ in LArTPC

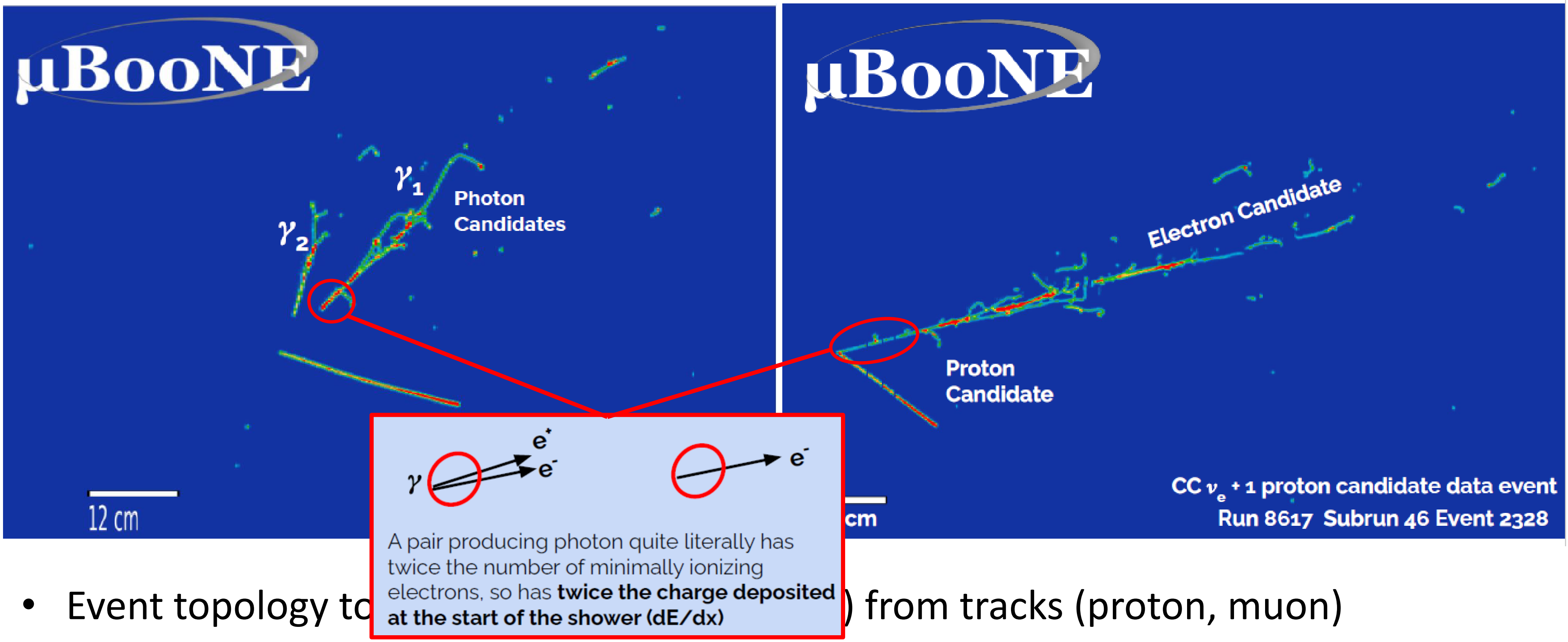

- Event topology to) from tracks (proton, muon)
- Separation of e and γ : Gap Identification + dE/dx
- Unique capability to identify ν_e charge-current (CC) interactions in LArTPC

Challenge in Automated Event Reconstruction

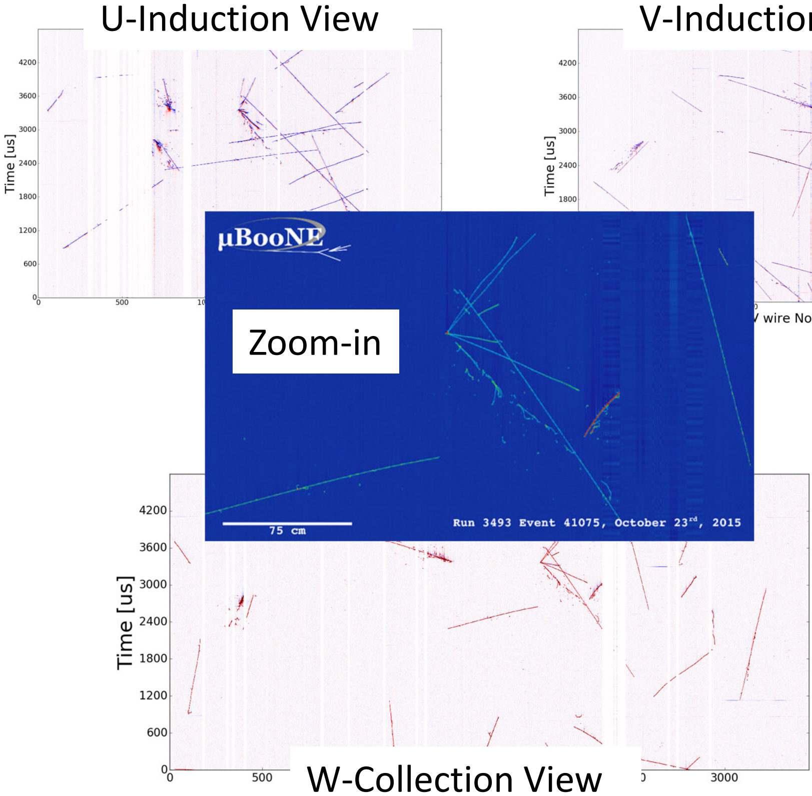

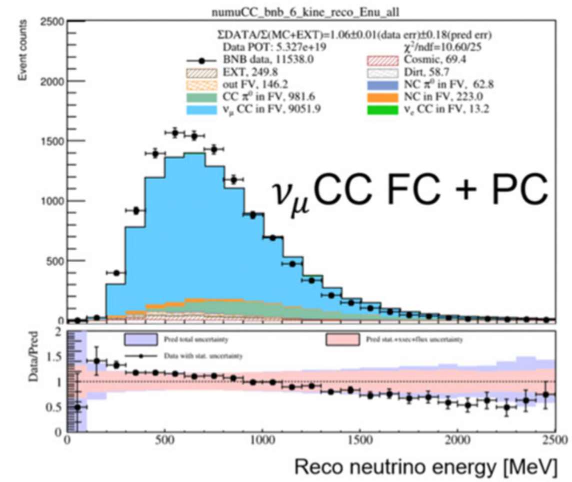

- How to convert the excellent resolution and calorimetry in these pictures to rigorous physics analyses?
  - Massive amount of information with tiny signal to background ratio → a big challenge for automated event reconstruction

Pandora Pattern Recognition

- The most general pattern recognition algorithm with the longest history
  - Eur. Phys. J. C78, 82 (2018)

MicroBooNE Publications Using Pandora

JINST 12 P12030 (2017);
Eur. Phys. J. C79: 248 (2019
PRD 99, 091102 (2019);
Eur. Phys. J. C79 673 (2019)
JINST 15, P03022 (2020);
JINST 15 P02007 (2020);
PRD 101, 052001 (2020);
PRL 125, 201803 (2020);
JINST 15, P12037 (2020);
PRD 102, 112013 (2020);

Track (p), daughter of primary p

Deep-Learning (DL) Based Event Reconstruction

- Currently a hybrid approach of Deep-Learning and traditional

Semantic Segmentation Using SparseSSNet (pixel-based

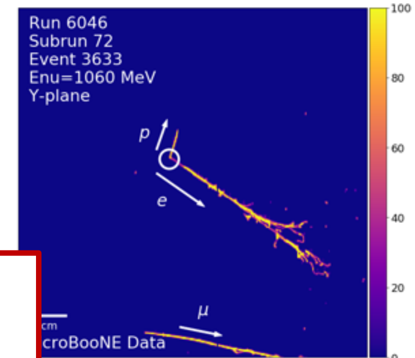

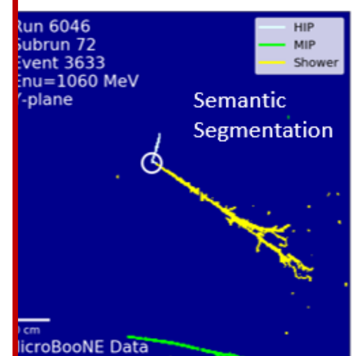

Wire-Cell Event Reconstruction

μBooNE

Wire-Cell

TPC simulation	3D imaging	3D trajectory & dQ/dx fitting	multi-track fitting
noise filtering	clustering	cosmic muon tagger	DL-3D vertexing
signal processing	charge-light matching		particle identification

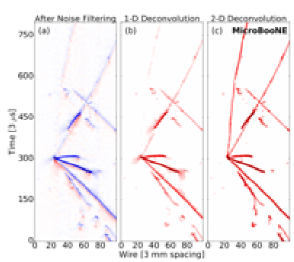

JINST 12 P08003 (2017)
JINST 13 P07006 (2018)
JINST 13 P07007 (2018)
JINST 16 P01036 (2020)

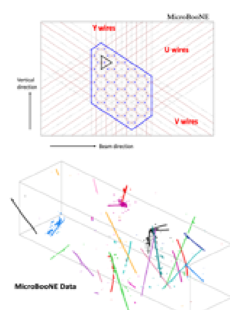

JINST 13 P05032 (2018)
JINST 16 P06043 (2021)

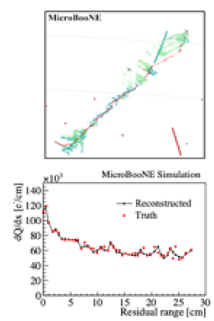

Phys. Rev. Applied 15 064071 (2021)
arXiv:2012.07928

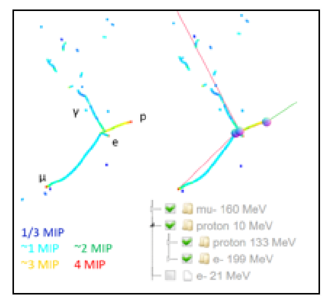

arXiv:2110.13961

201 collaborators, 36 institutions, 5 countries

MicroBooNE collaboration @ 2016

MicroBooNE Detector: An 85-ton LArTPC

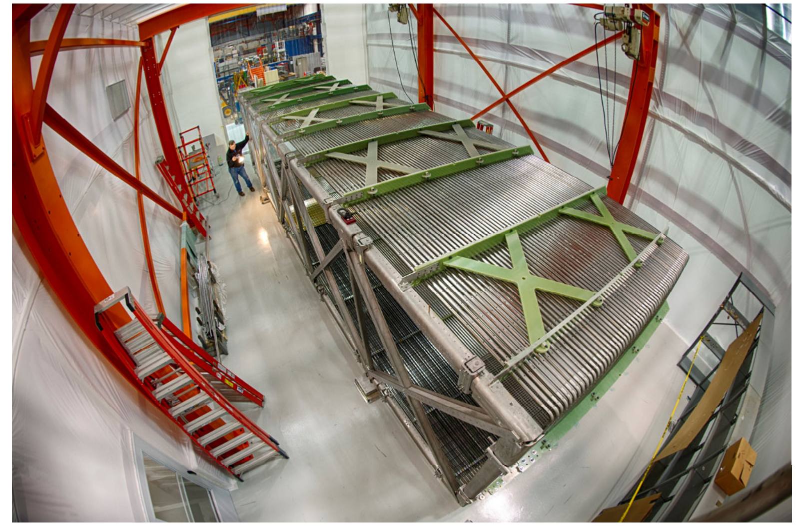

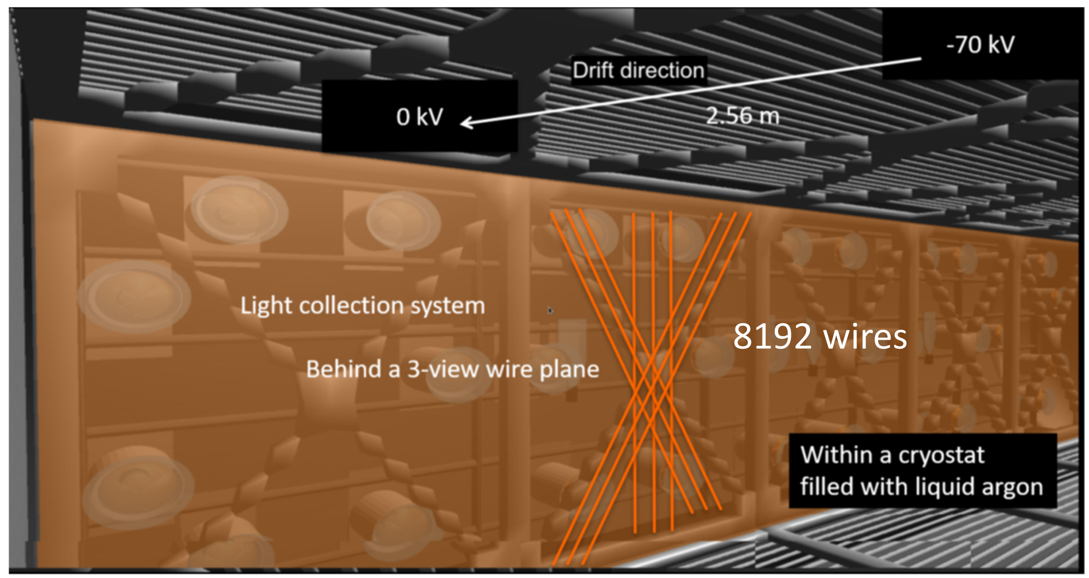

Fermilab

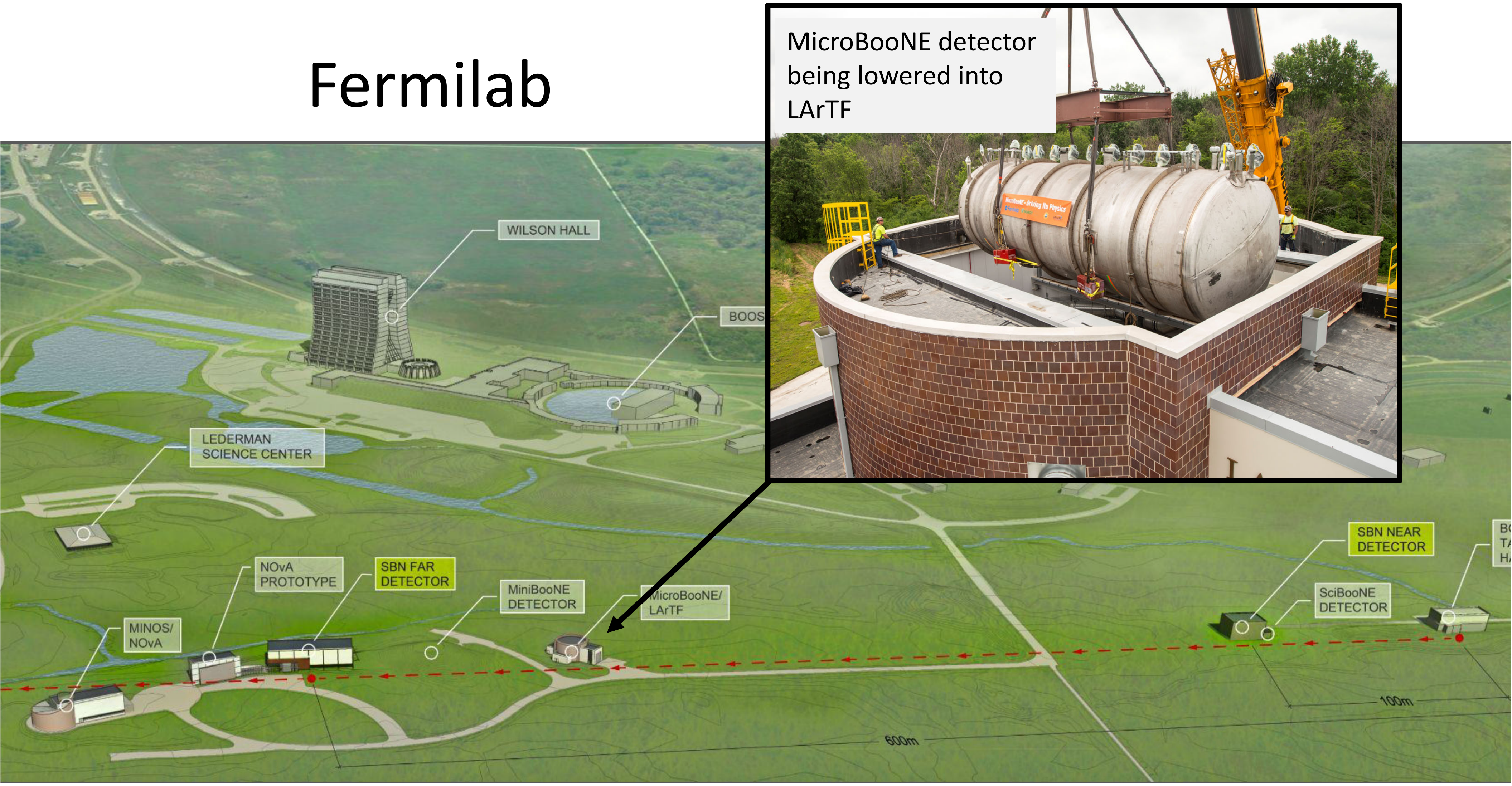
MicroBooNE detector being lowered into LArTF
WILSON HALL
LEDERMAN SCIENCE CENTER
NOvA PROTOTYPE
SBN FAR DETECTOR
MiniBooNE DETECTOR
MicroBooNE/ LArTF
MINOS/ NOvA
SBN NEAR DETECTOR
SciBooNE DETECTOR
100m
600m

Booster Neutrino Beamline

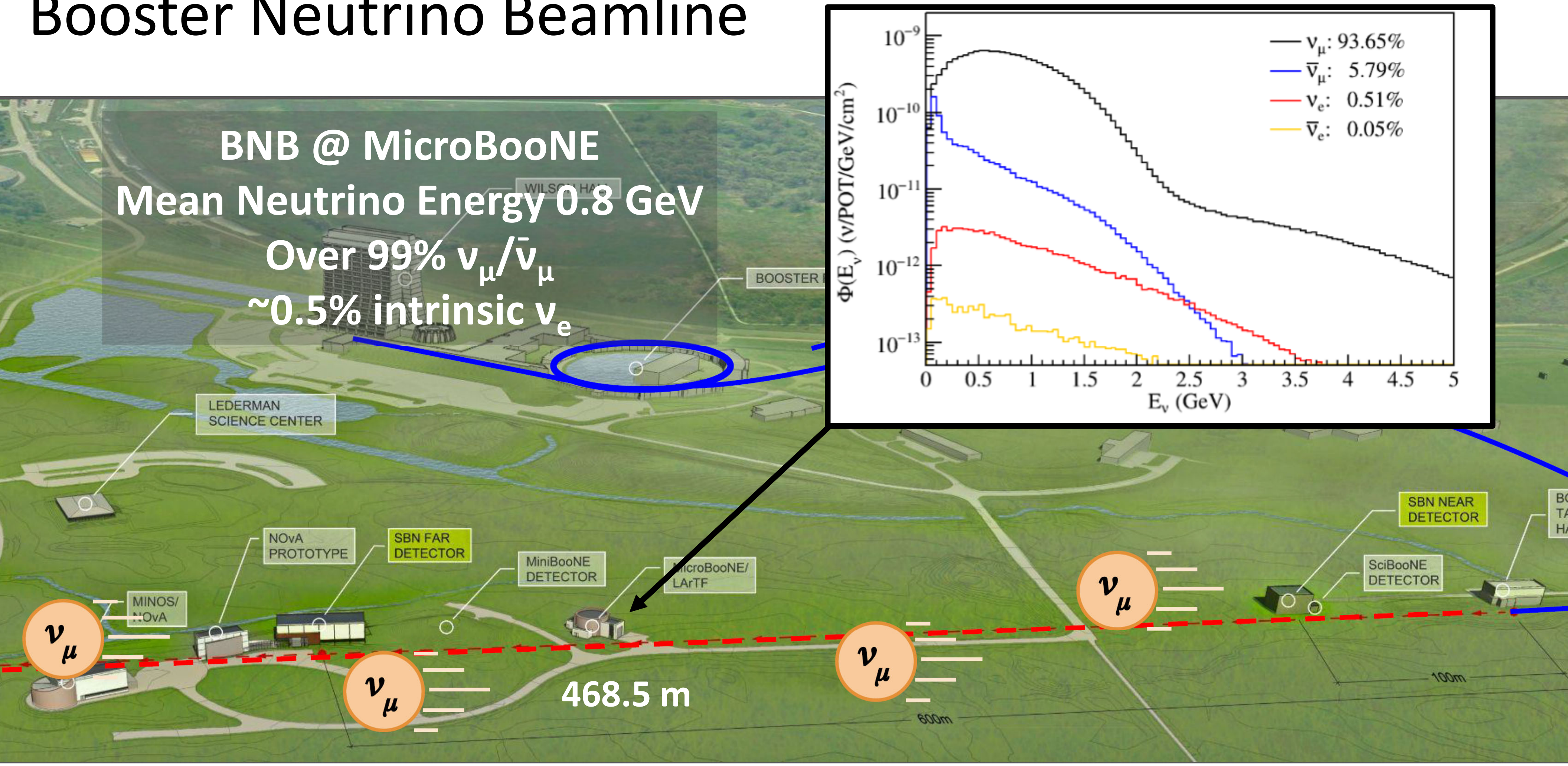

Booster Neutrino Beamline

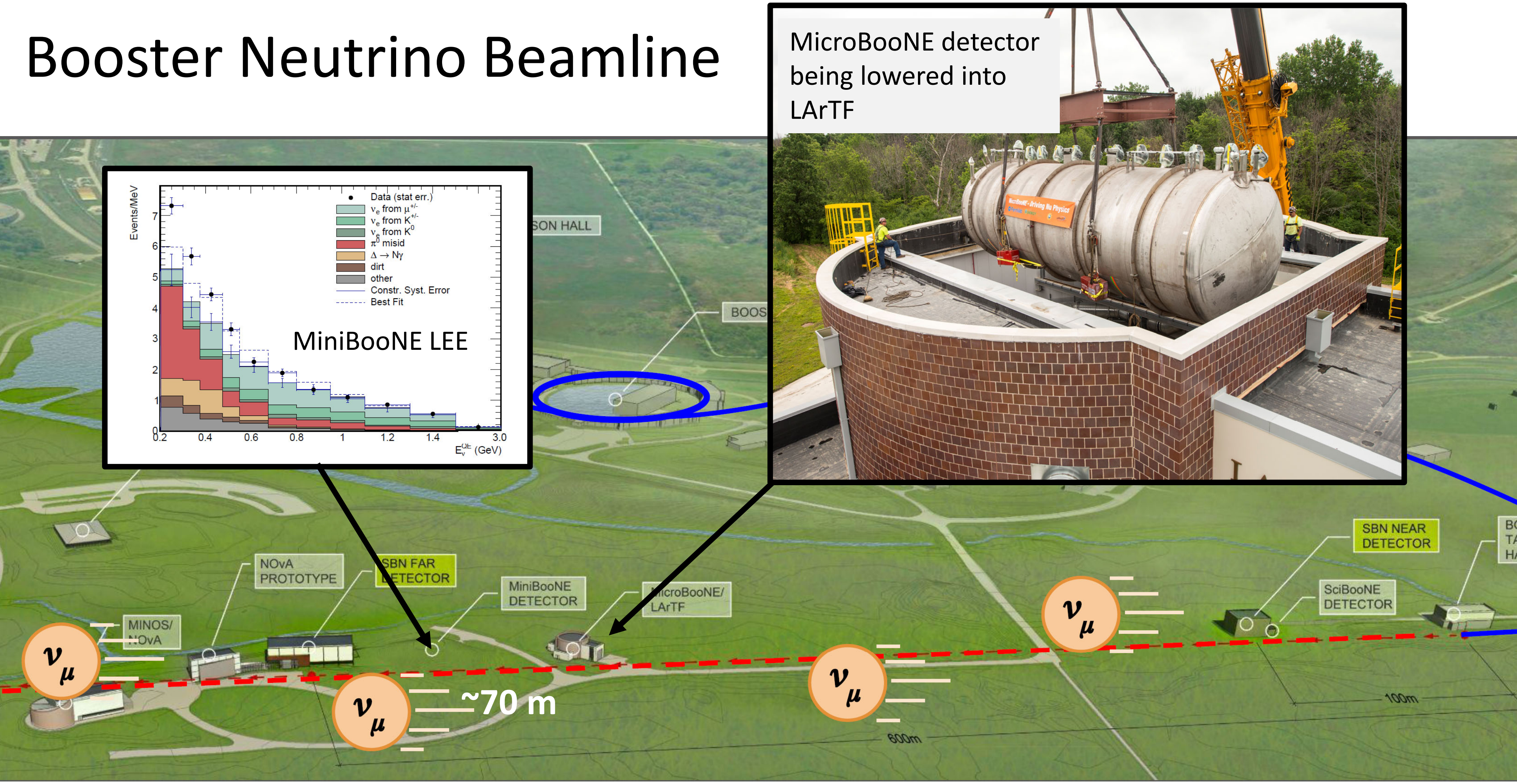

MicroBooNE Science Goals (Physics + R&D)

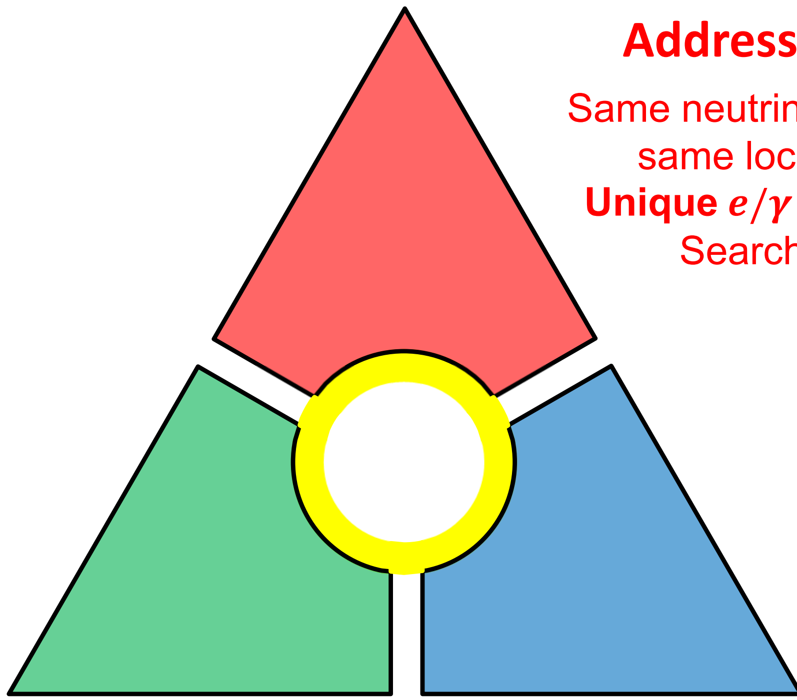

Address MiniBooNE LEE

Same neutrino beamline and roughly same location as MiniBooNE
Unique e/γ separation capability
Search for BSM physics

LArTPC hardware & software R&D

LArTPC design, cryostat, cold electronics ...
Noise filtering, TPC signal processing, detector physics,
event reconstruction

Study ν-Ar interactions

Inclusive & exclusive cross section measurements,
Validation of modeling of neutrino energy

Largest Sample of neutrino interactions on argon in the world

2015-10-15 first beam

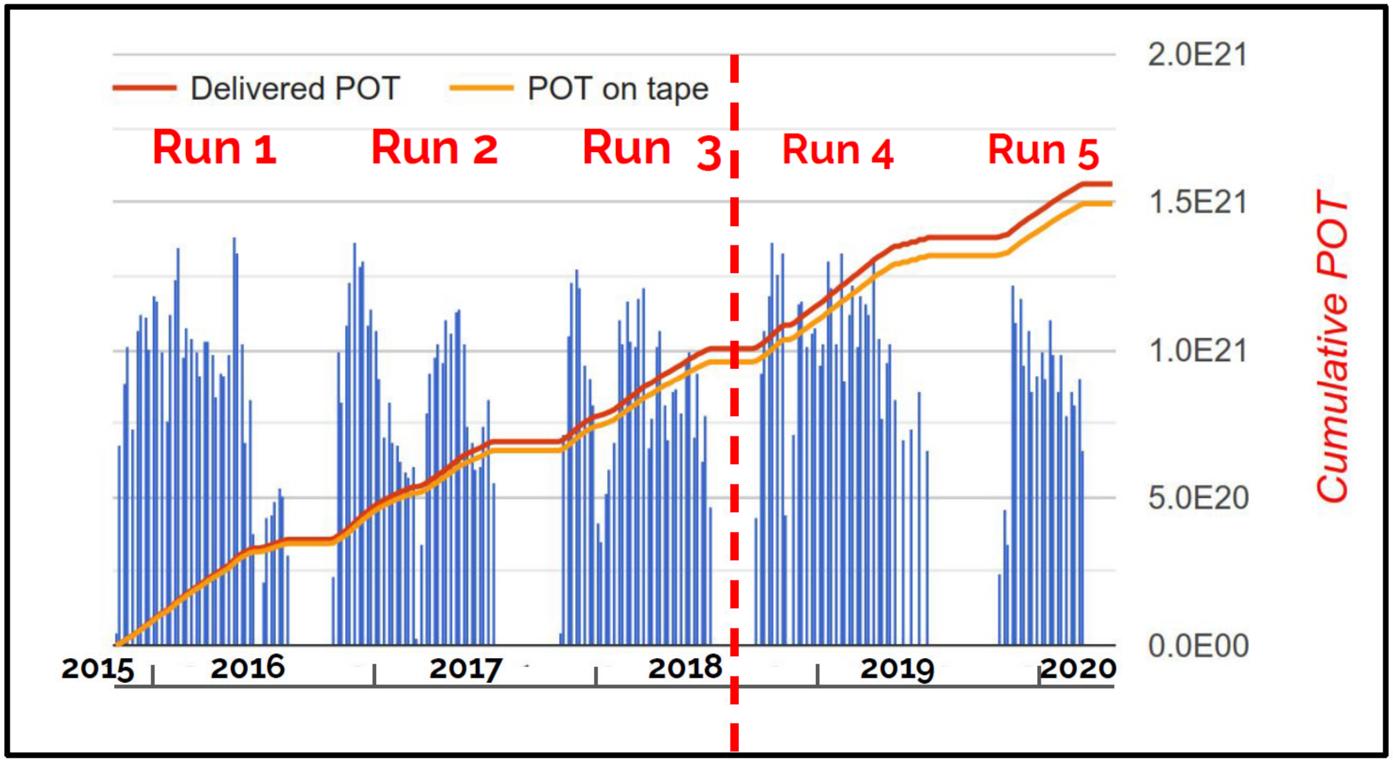

Recent physics results are based on ~7e20 protons-on-target from run 1 - 3

Wire-Cell Event Reconstruction

TPC simulation noise filtering signal processing	3D imaging clustering charge-light matching	3D trajectory & dQ/dx fitting cosmic muon tagger	multi-track fitting DL-3D vertexing particle identification

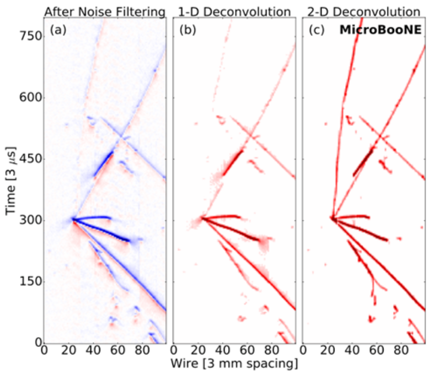

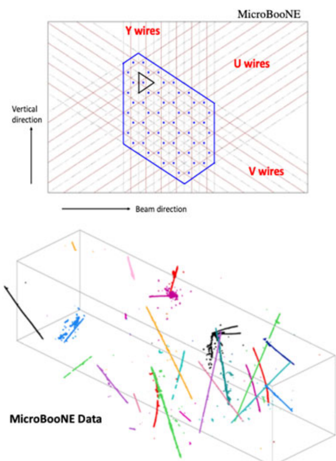

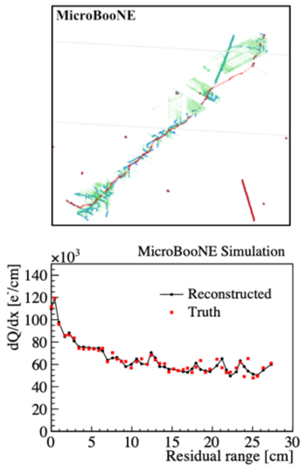

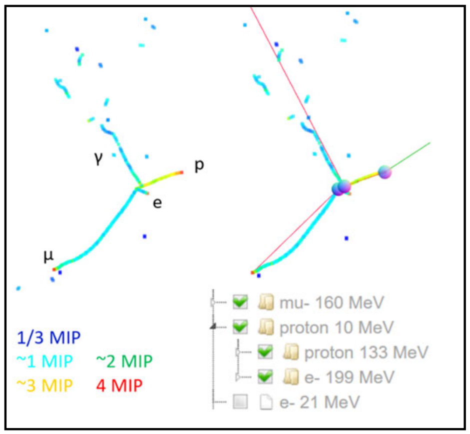

JINST 12 P08003 (2017)
JINST 13 P07006 (2018)
JINST 13 P07007 (2018)
JINST 16 P01036 (2020)

JINST 13 P05032 (2018)
JINST 16 P06043 (2021)

Phys. Rev. Applied 15 064071 (2021)
arXiv:2012.07928

arXiv:2110.13961

Complex TPC Charge Signal

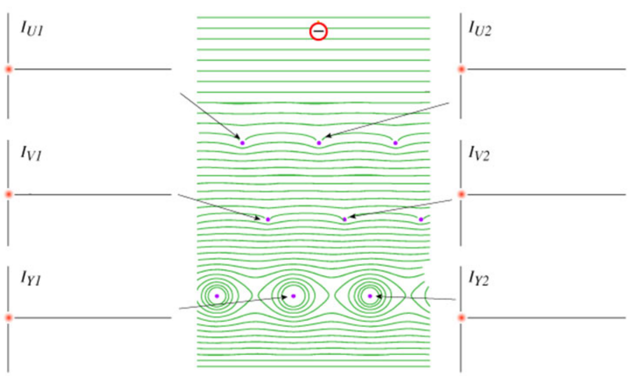

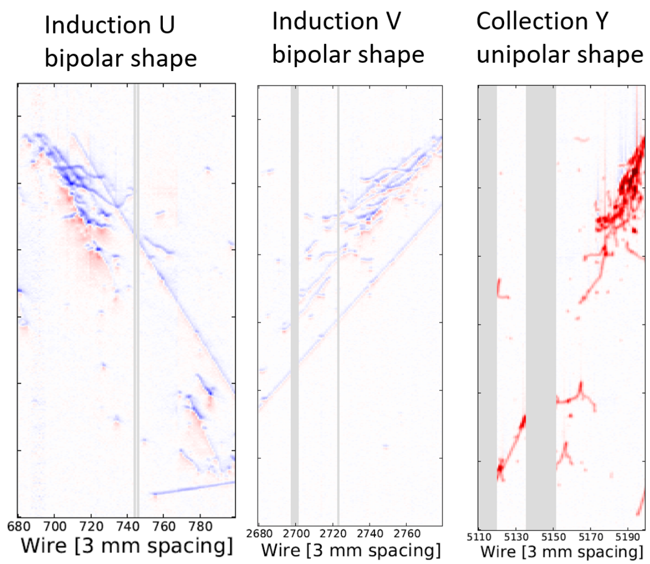

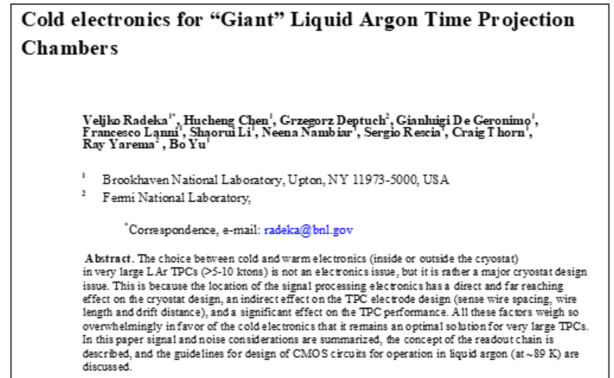

Cold electronics for "Giant" Liquid Argon Time Projection Chambers

Veljko Radeka[1*], Hucheng Chen[1], Grzegorz Deptuch[2], Gianluigi De Geronimo[1], Francesco Lanni[1], Shaorui Li[1], Neena Nambiar[1], Sergio Rescia[1], Craig Thorn[1], Ray Yarema[2], Bo Yu[1]

[1] Brookhaven National Laboratory, Upton, NY 11973-5000, USA
[2] Fermi National Laboratory,

*Correspondence, e-mail: radeka@bnl.gov

Abstract. The choice between cold and warm electronics (inside or outside the cryostat) in very large LAr TPCs (>5-10 ktons) is not an electronics issue, but it is rather a major cryostat design issue. This is because the location of the signal processing electronics has a direct and far reaching effect on the cryostat design, an indirect effect on the TPC electrode design (sense wire spacing, wire length and drift distance), and a significant effect on the TPC performance. All these factors weigh so overwhelmingly in favor of the cold electronics that it remains an optimal solution for very large TPCs. In this paper signal and noise considerations are summarized, the concept of the readout chain is described, and the guidelines for design of CMOS circuits for operation in liquid argon (at ~89 K) are discussed.

1st International Workshop towards the Giant Liquid Argon Charge Imaging Experiment (2011)

JINST 12 P08003

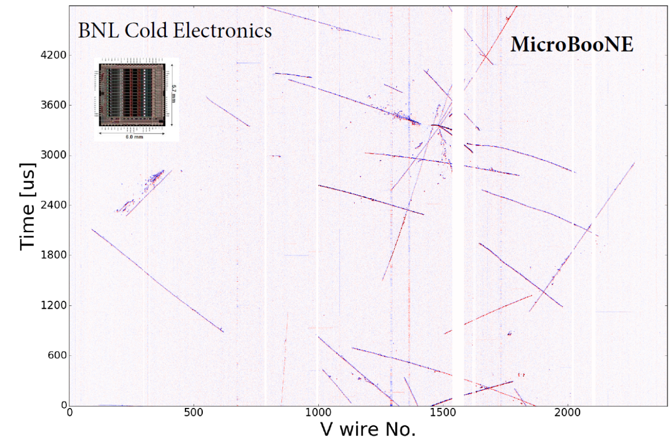

- An enabling technology: cold electronics
  - Placing the preamplifier inside LAr significantly reduced the electronics noise

TPC Signal Processing → Recover (or Unfold) Ionization Electrons

Time domain

$$\mathrm{M}(t_0) = \int_t R(t - t_0) \cdot S(t) \cdot dt$$

Fourier transformation

$$M(\omega) = \mathrm{R}(\omega) \cdot \mathrm{S}(\omega)$$

Frequency domain

$$\mathrm{S}(\omega) = \frac{\mathrm{M}(\omega)}{\mathrm{R}(\omega)} \cdot F(\omega)$$

Back to time domain

Inverse-Fourier transformation

$$\mathrm{S(t)}$$

- Signal processing is based on deconvolution technique
  - $O(N^3)$ matrix inversion is achieved through a O(N logN) fast Fourier transformation
    - Top 10 algorithms in 20^{th} century

- 1-D deconvolution described in B. Baller "Liquid Argon TPC Signal Formation, Signal Processing, and reconstruction techniques", JINST 12, P07010

2-D Deconvolution

$$M_i(t_0) = \int_t \left(R_0(t-t_0)\cdot S_i(t) + R_1(t-t_0)\cdot S_{i+1}(t) + \ldots \right) \cdot dt$$

$$M_i(\omega) = R_0(\omega)\cdot S_i(\omega) + R_1(\omega)\cdot S_{i+1}(\omega) + \ldots$$

$$\begin{pmatrix} M_1(\omega) \\ M_2(\omega) \\ \ldots \\ M_{n-1}(\omega) \\ M_n(\omega) \end{pmatrix} = \begin{pmatrix} R_0(\omega) & R_1(\omega) & \ldots & R_{n-2}(\omega) & R_{n-1}(\omega) \\ R_1(\omega) & R_0(\omega) & \ldots & R_{n-3}(\omega) & R_{n-2}(\omega) \\ \ldots & \ldots & \ldots & \ldots & \ldots \\ R_{n-2}(\omega) & R_{n-3}(\omega) & \ldots & R_0(\omega) & R_1(\omega) \\ R_{n-1}(\omega) & R_{n-2}(\omega) & \ldots & R_1(\omega) & R_0(\omega) \end{pmatrix} \cdot \begin{pmatrix} S_1(\omega) \\ S_2(\omega) \\ \ldots \\ S_{n-1}(\omega) \\ S_n(\omega) \end{pmatrix}$$

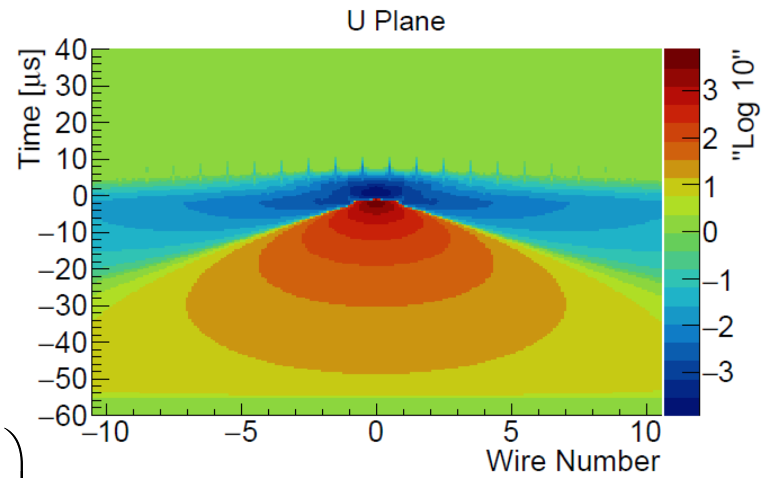

Position-dependent responses

The inversion of matrix R can again be done with deconvolution through 2-D Fast Fourier Transformation

Also, Region of Interest (ROI) is essential to deal with the induction wire plane signal

- With induced signals, the signal is still linear summation
  - R_1 represents the induced signal from i+1th wire signal to ith wire
  - S_i and S_{i+1} are not directly related

Improved TPC Signal Processing

1D deconvolution

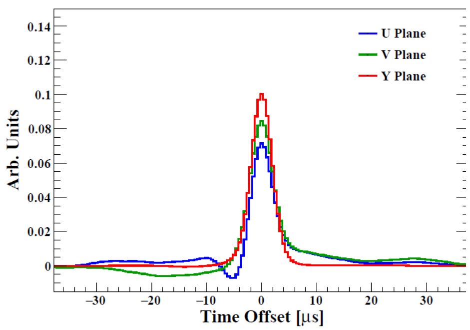

2D deconvolution

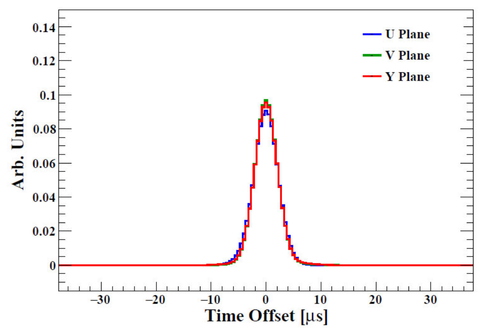

The 2D deconvolution algorithm in Wire-Cell allows to accurately recover the ionization electrons from recorded original signals

Same number of electrons are reconstructed from each projection wire plane

Original

1D deconvolution

2D deconvolution

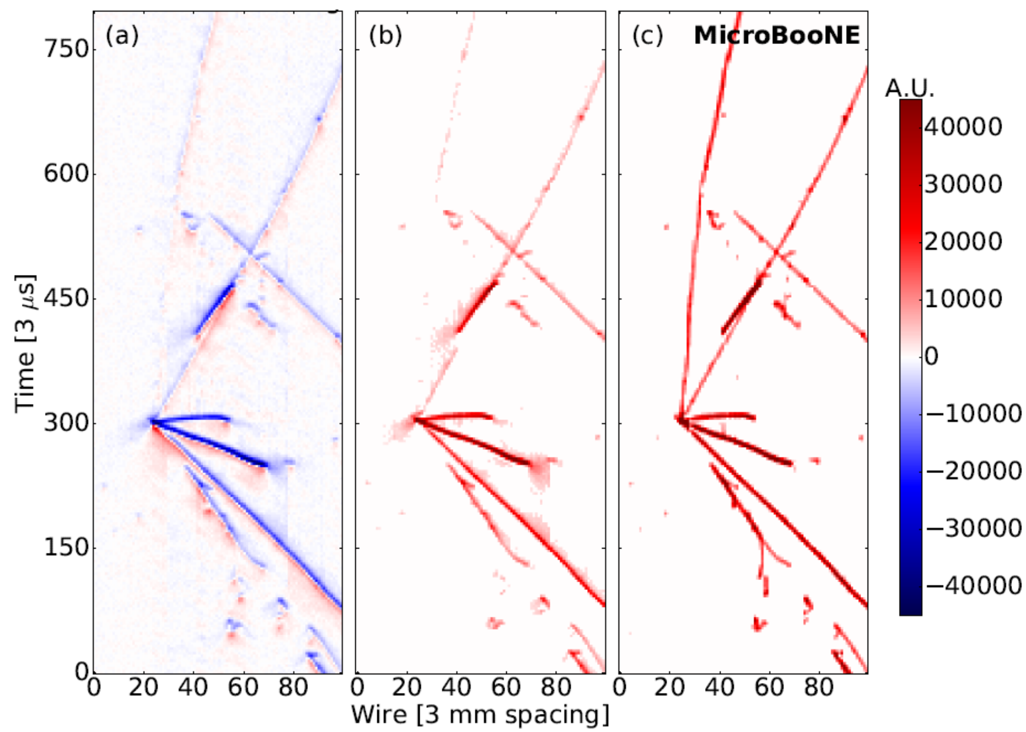

[JINST 13 P07006/7](https://doi.org/10.1088/1748-0221/13/07/P07006)

Wire-Cell Tomographic Event Reconstruction

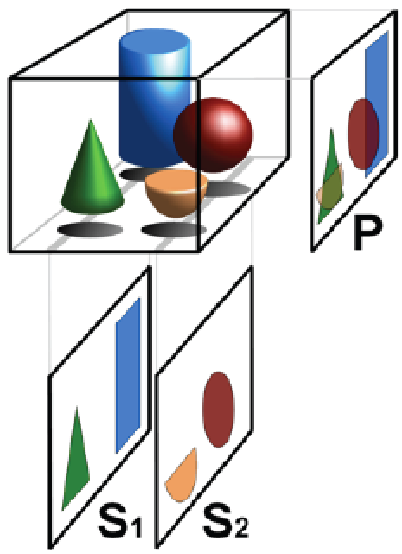

Fig.1:Basic principle of tomography: superposition free tomographic cross sections S1 and S2 compared with the projected image P

https://en.wikipedia.org/wiki/Tomography

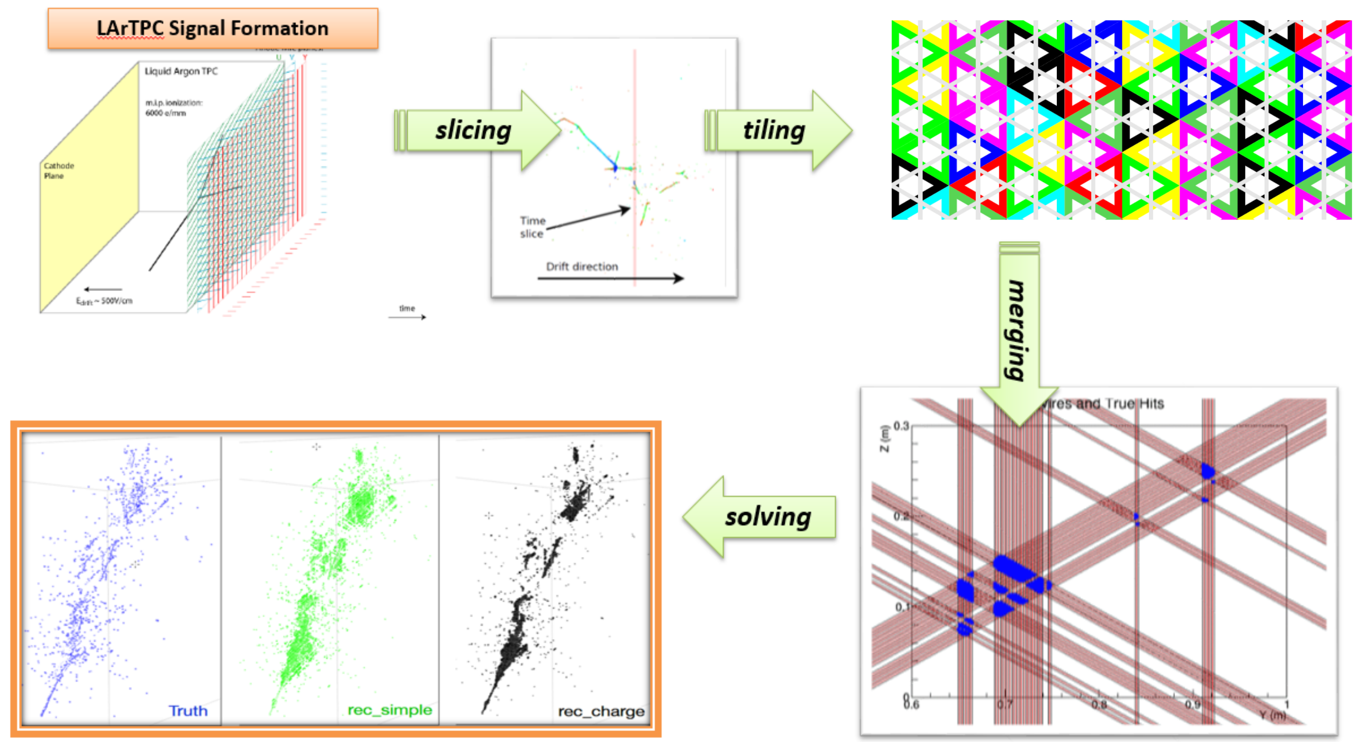

“Three-dimensional Imaging for Large LArTPCs”, XQ, C. Zhang, B. Viren, M. Diwan, [JINST 13, P05032 (2018)]

Traditional Reconstruction Approach: 2D matching → 3D

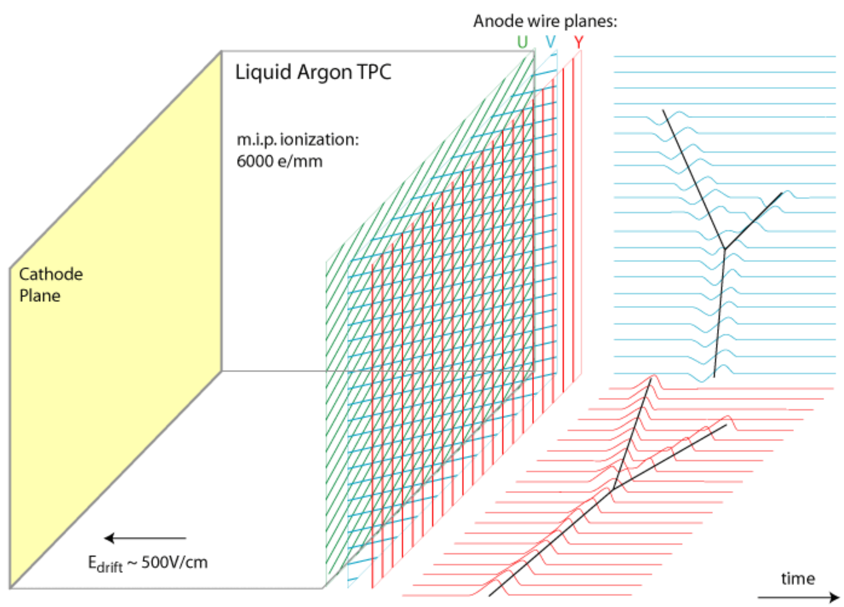

2D pattern recognition

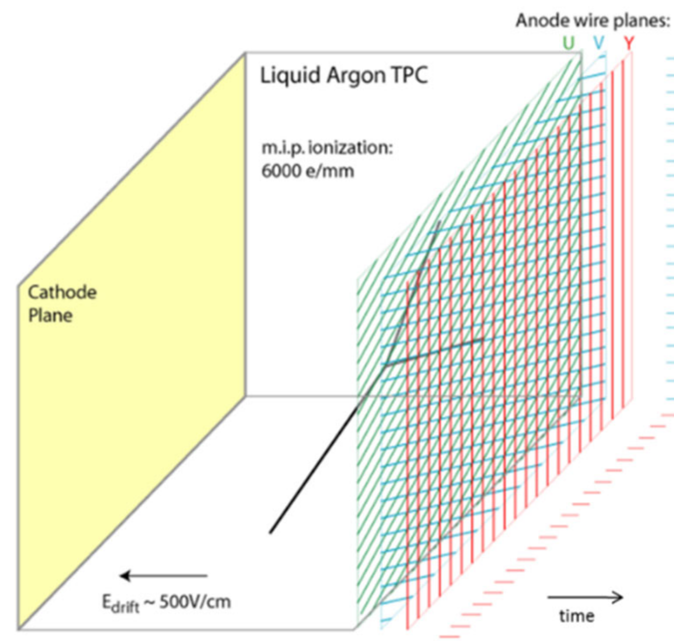

Matching to 3D objects

Error made in pattern recognition will propagate to the later reconstruction steps

Solving: usage of Charge, Sparsity, Positivity, Connectivity

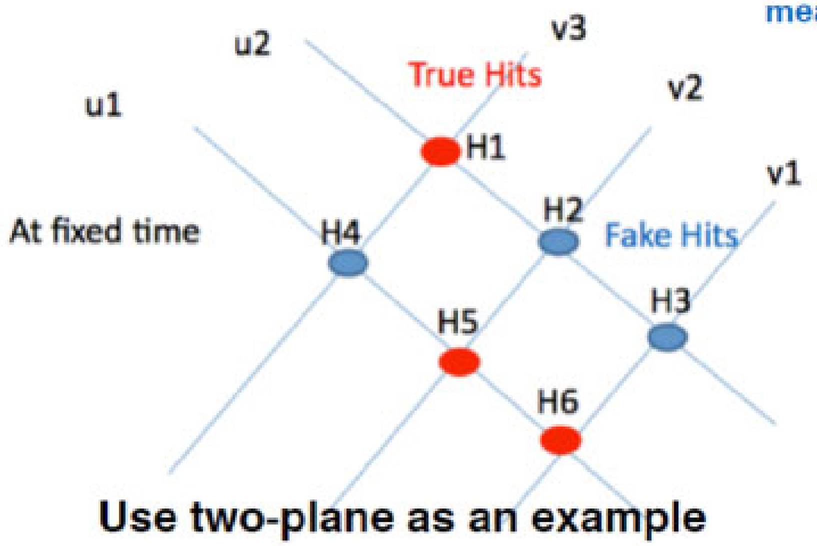

measured charges on wires

true charges to be solved

$$\begin{pmatrix} u1 \\ u2 \\ v1 \\ v2 \\ v3 \end{pmatrix} = \begin{pmatrix} 0 & 0 & 0 & a & a & a \\ a & a & a & 0 & 0 & 0 \\ 0 & 0 & a & 0 & 0 & a \\ 0 & a & 0 & 0 & a & 0 \\ a & 0 & 0 & a & 0 & 0 \end{pmatrix} \cdot \begin{pmatrix} H_1 \\ H_2 \\ H_3 \\ H_4 \\ H_5 \\ H_6 \end{pmatrix}$$

Matrix determined by geometry

(a=1)

$$y = Ax$$

- The goal is to differentiate the true hits from fake ones by using the charge information
  - ~ large charge → true hits ~ zero charge → fake hits
- Sparsity, positivity, and connectivity information are added through compressed sensing (L1 regularization)

L1 reg. $O(N!) \rightarrow O(m \times N)$

$$\chi^2 = (y - A \cdot x)^2 + \lambda \cdot \sum_i |x_i|$$

E. Candes, J. Romberg, T. Tao arXiv-math/0503066

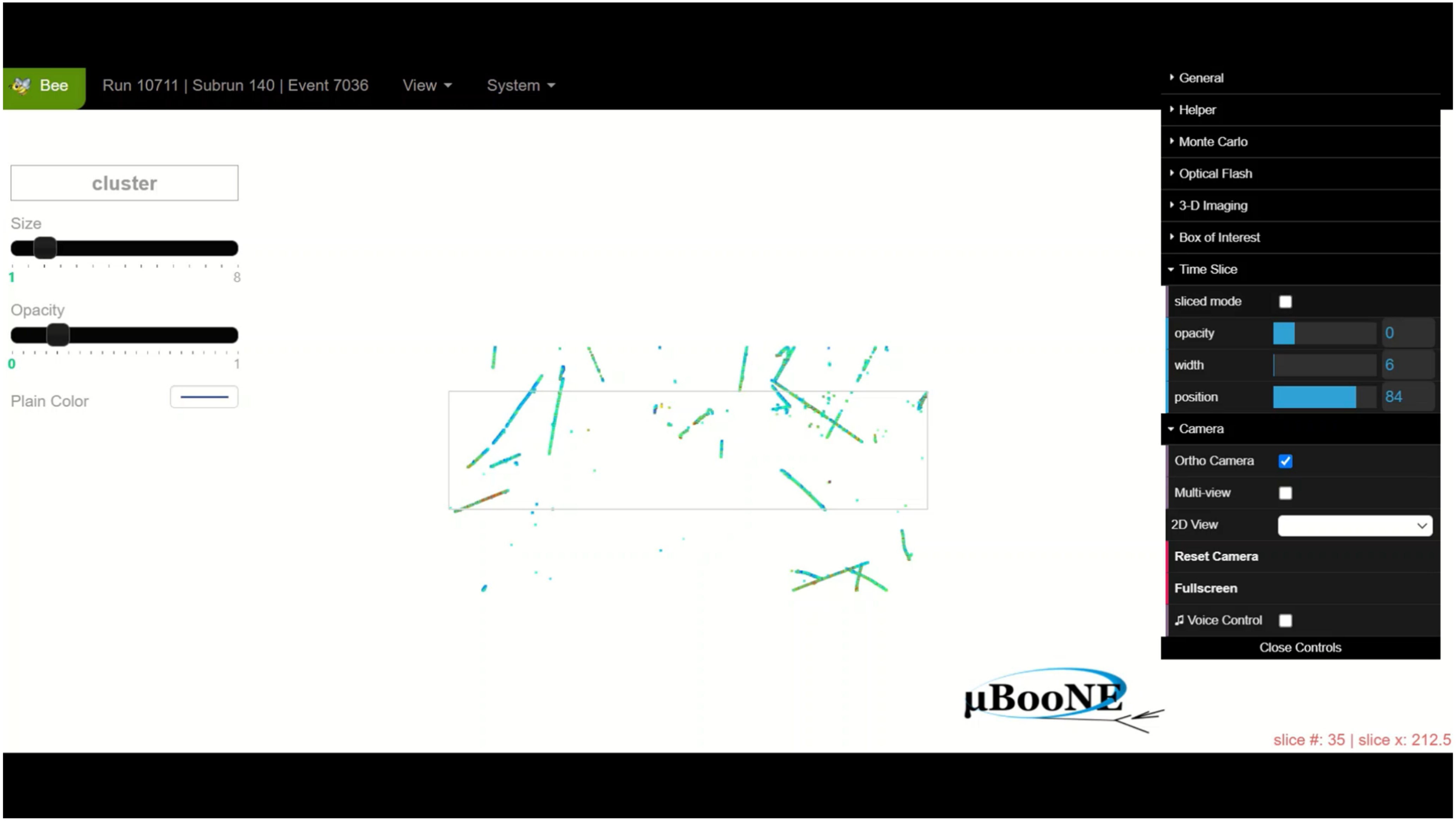
Bee
Run 10711 | Subrun 140 | Event 7036
View
System
cluster
Size
1
8
Opacity
0
1
Plain Color
General
Helper
Monte Carlo
Optical Flash
3-D Imaging
Box of Interest
Time Slice
sliced mode
opacity
0
width
6
position
84
Camera
Ortho Camera
Multi-view
2D View
Reset Camera
Fullscreen
Voice Control
Close Controls
µBooNE
slice #: 35 | slice x: 212.5

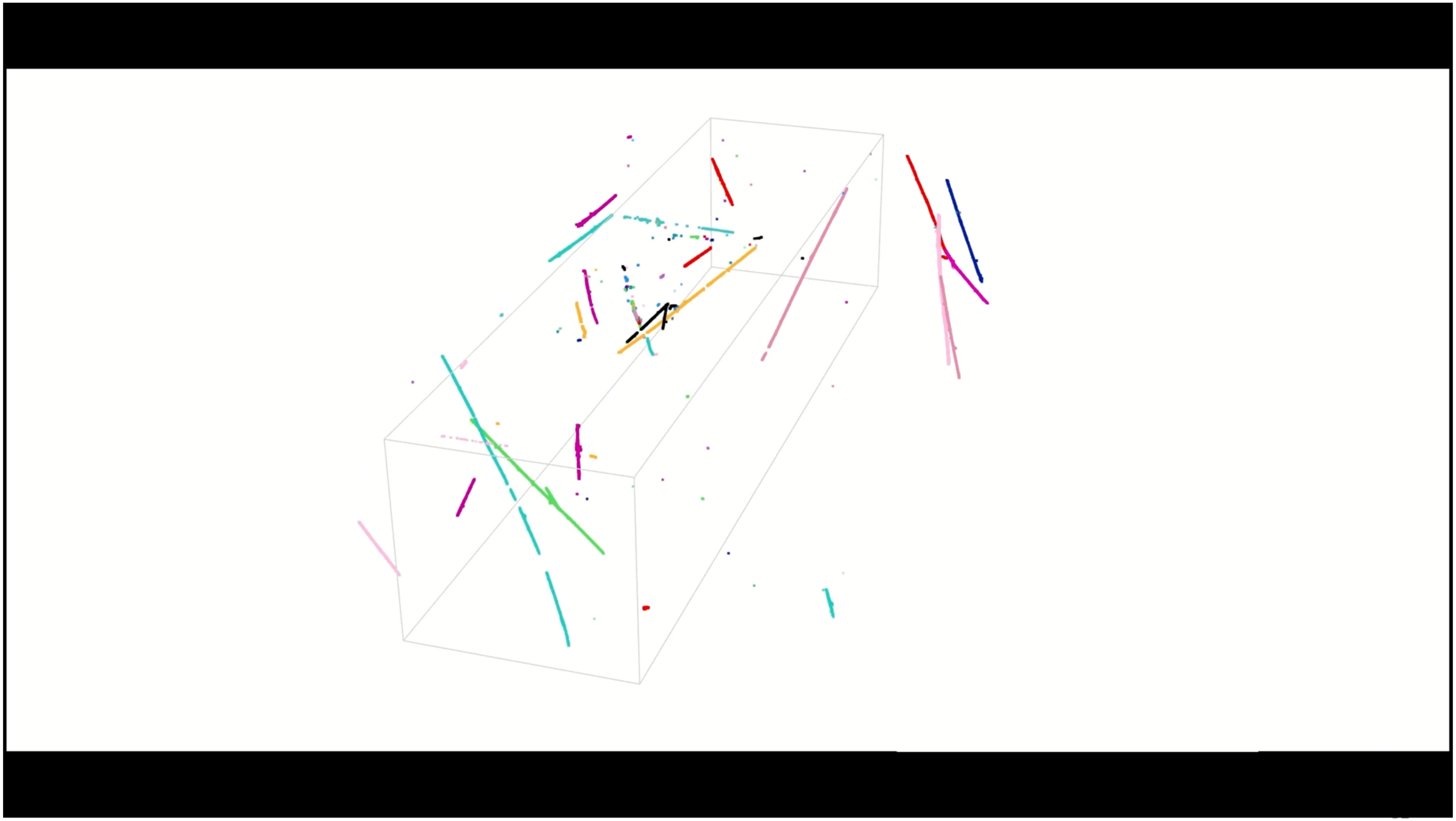

Matching Principle

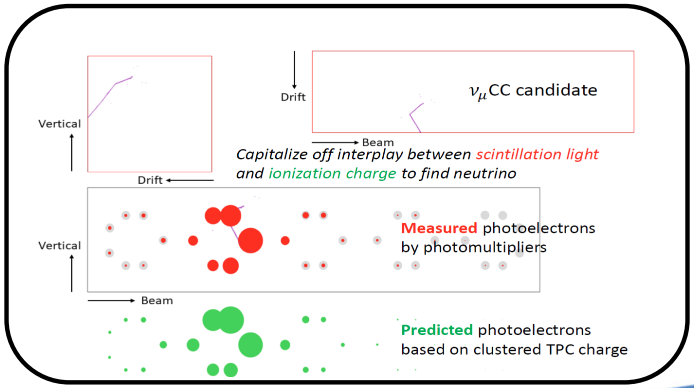

Recognized clusters with different colors

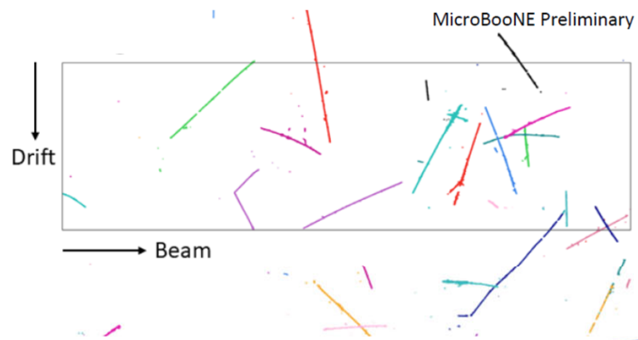

4.8 ms drift window

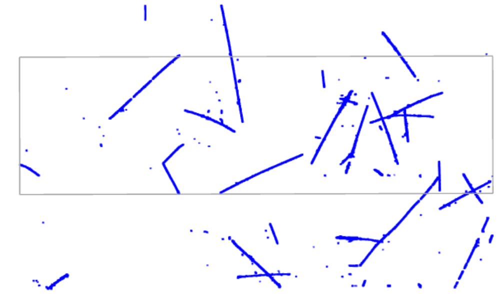

20-30 TPC activities

- **Light signal proportional to (reconstructed 3D) charge**
- Known light acceptance given position
- Predicted vs. Measured light pattern with Compressed Sensing

All possible hypotheses

- One flash → <u>many or zero</u> TPC clusters within corresponding active volume (activities in inactive volume)
- One cluster → <u>at most one flash</u> (inefficiency in the light system)

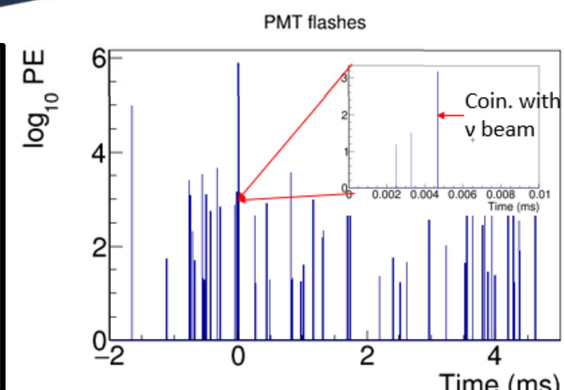

40-50 PMT activities

Rejecting Through-Going Muons (TGM)

- Only event with flash(light) time matching the neutrino beam spill window is a neutrino candidate

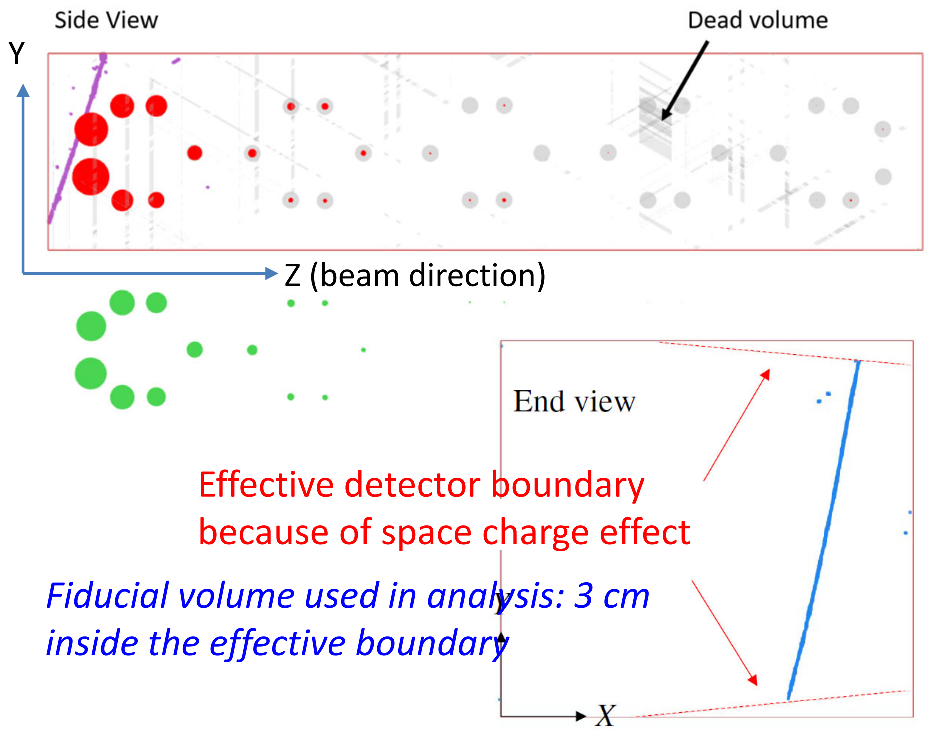

- TGM: cosmic-ray muons go all way through the active TPC volume

- Identification: the two endpoints of TPC cluster at/outside the effective detector boundary

	Neutrino:Cosmic-ray	
Charge-light matching	1 : 6.4	Improved by factor of 6
TGM rejection	1 : 0.9	

Rejecting Stopping Muons

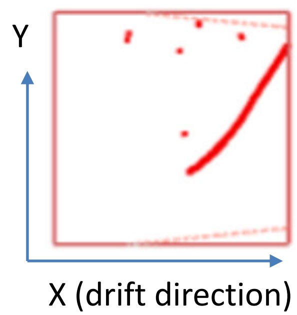

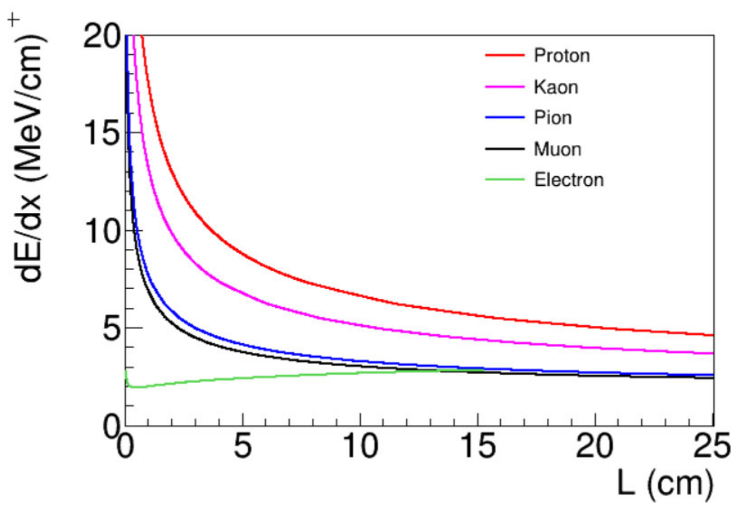

- STM: cosmic-ray muons enter and stop inside the active volume

- Identified by directionality: from outside to inside
  - Tracks from neutrino activities will go out of detector from inside
  - Tracks from background will enter the detector from outside
- Trajectory and dQ/dx fitting → Bragg peak → directionality
- dQ/dx vs. residual range is also important for the particle identification for tracks

Principle of the Fit

- Come up with a 3D track hypothesis (3D trajectory points and dQ/dx)
- Predict the deconvolved signals on all projection views
- Minimize the difference between the observation and prediction

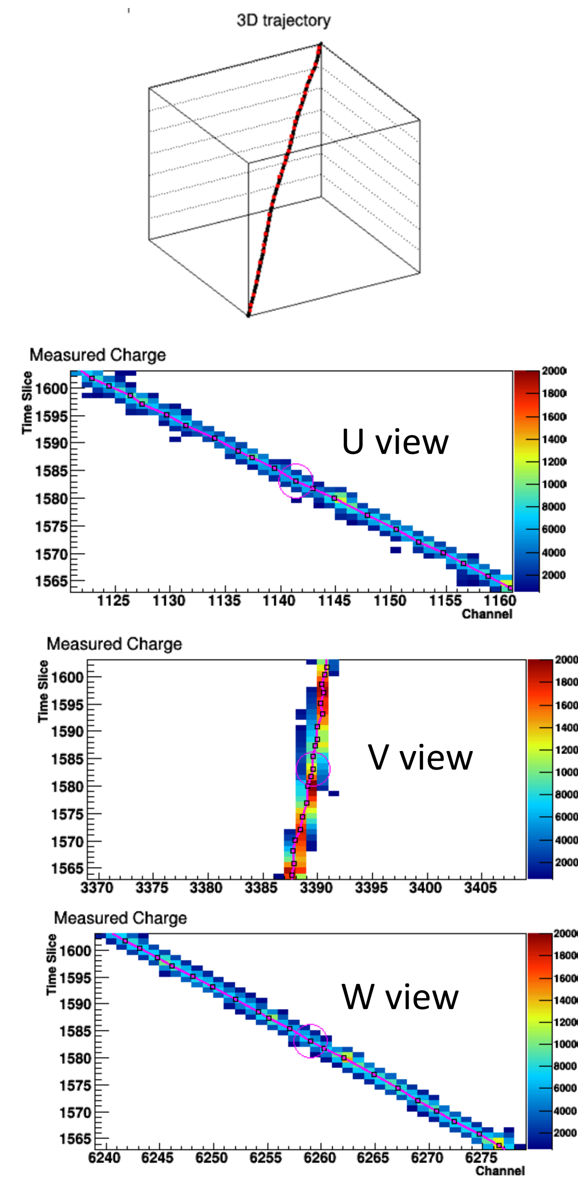

Simplified Prediction of the Deconvolved Signal

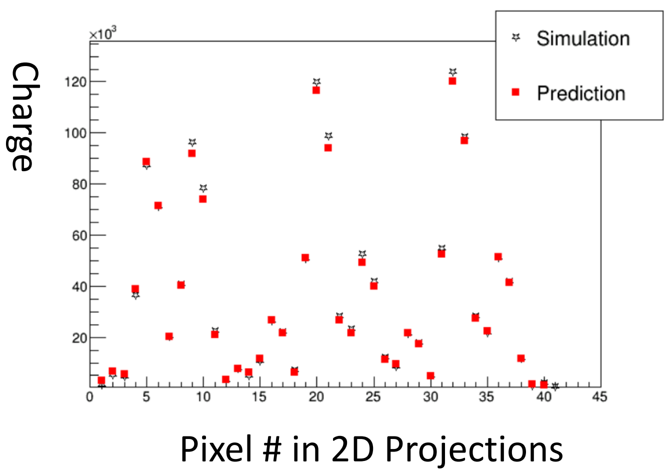

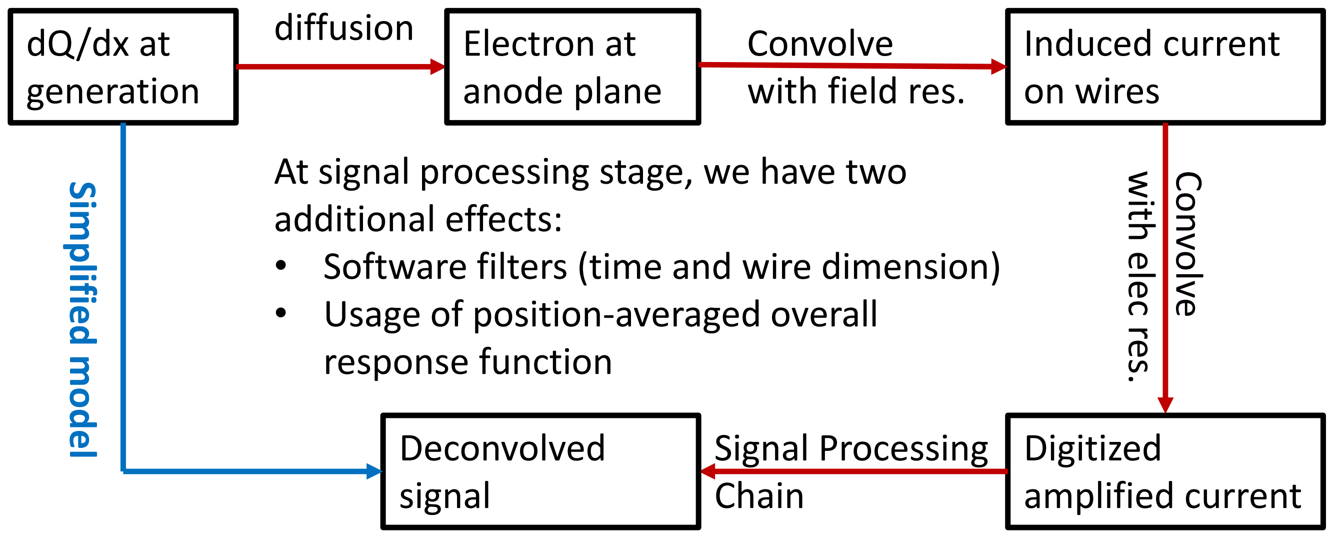

- Full process of signal formation and signal processing is complex → significant burden in computation
- A simplified model was developed

Trajectory and dQ/dx Fitting

Overall Test Statistics

$$T\left(x_j, y_j, z_j, Q_j\right) = T_U + T_V + T_W + T_{reg}$$

$$\mathrm{T}_{U/V/W} = \sum_j \sum_i \frac{q_i^2}{\delta q_i^2} \cdot dis\left(U/V/W\right)_{ij}^2$$

Unknowns

Measurements

i : pixel in 2D projection j : 3D trajectory point

$$dis(U)_{ij}^2 = \Delta U^2 \cdot \left(U_i - U_j\left(x_j, y_j, z_j\right)\right)^2 + \Delta x^2 \cdot \left(t_i - t_j\left(x_j, y_j, z_j\right)\right)^2$$

ΔU: bin size in U view, Δx : bin siz in drift time t

Overall Test Statistics

$$T\left(x_j, y_j, z_j, Q_j\right) = T_U + T_V + T_W + T_{reg}$$

$$T_U = \sum_{i=U,T} \frac{\left(q_i - \sum_j R_{Uij} Q_j\right)^2}{\delta q_i^2},$$

R_{Uij} : smearing coefficients

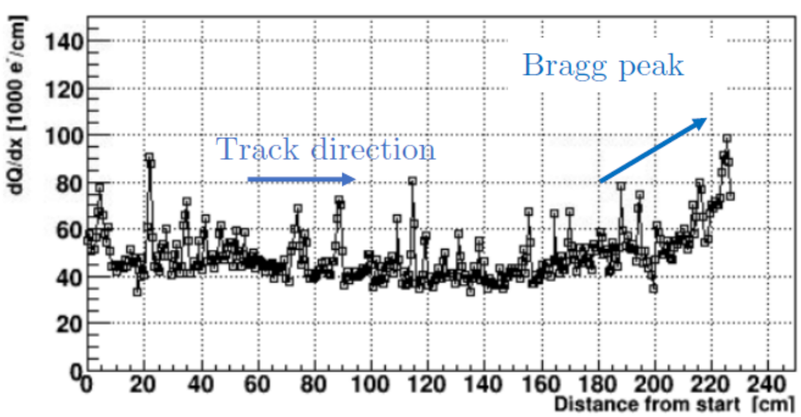

	Neutrino:Cosmic-ray	
Charge-light matching	1 : 6.4	Improved by factor of >6
TGM rejection	1 : 0.91	
STM rejection	1 : 0.36	Improved by factor of ~3
Additional Cuts	1 : 0.20	

Preselection

- Generic neutrino detection powered by many-to-many charge light matching and additional cosmic taggers to reject in-time coincidence cosmic-ray muons
  – 99.999% cosmic-ray muon background rejected
    - Start with 1:20,000 neutrinos to cosmics
    - End with 5.2:1 neutrinos to cosmics
  – 90% efficiency for ν_eCC and 80% efficiency for ν_μCC
  – ν_eCC purity ~0.4% at this stage

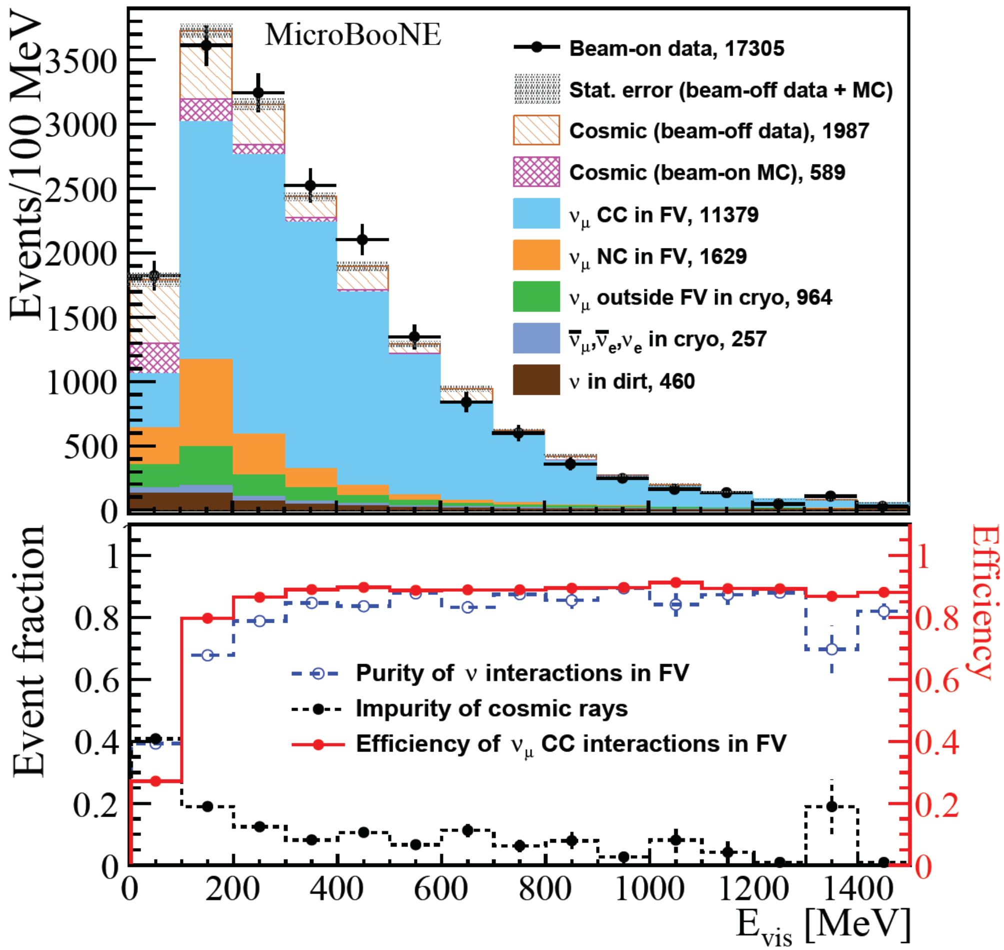

Phys. Rev. Applied 15, 064071

3D Pattern Recognition

(a) Selected neutrino activity

(b) Track/Shower separation

(c) Particle-level sub-clustering

(d) 3D dQ/dx displayed with PID capability

(e) Particle flow starting from neutrino vertex

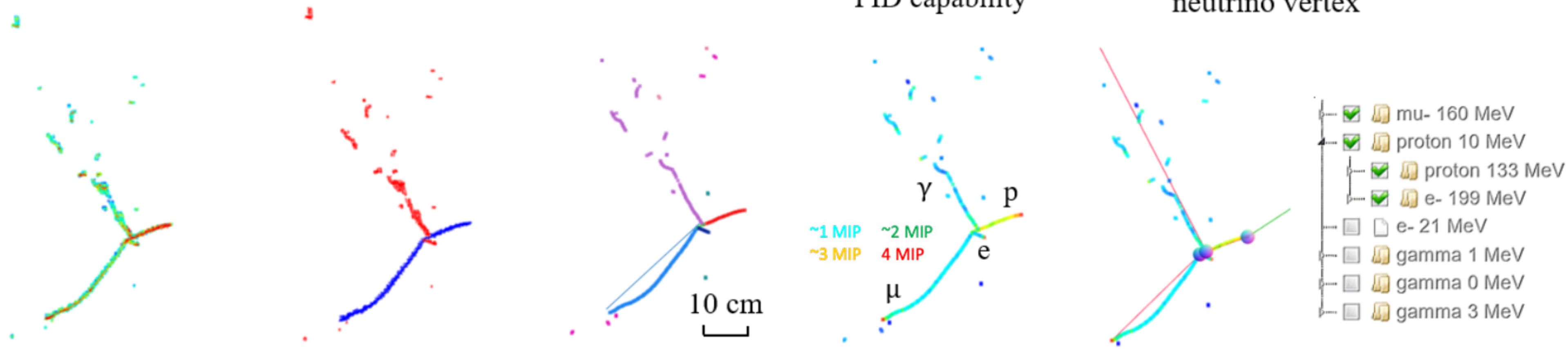

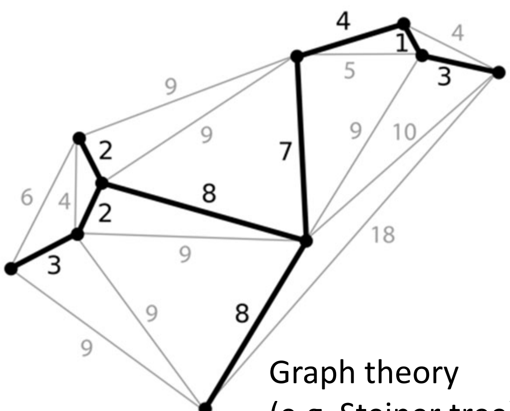

Graph theory
(e.g. Steiner tree)

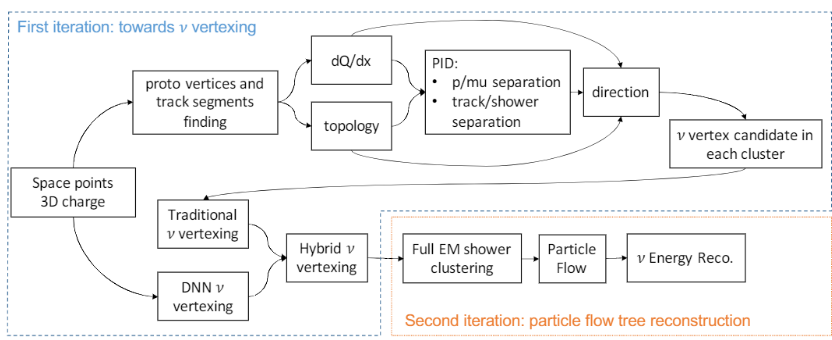

Deep-learning neural network

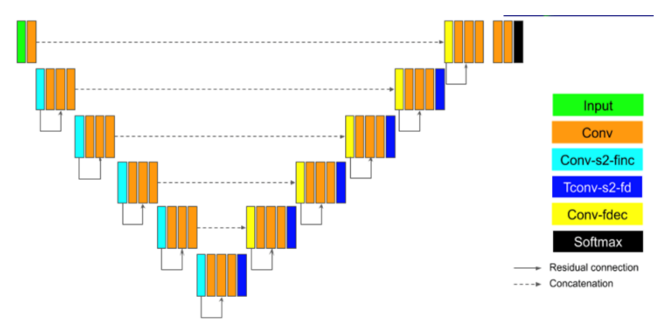

Neutrino Energy Reconstruction

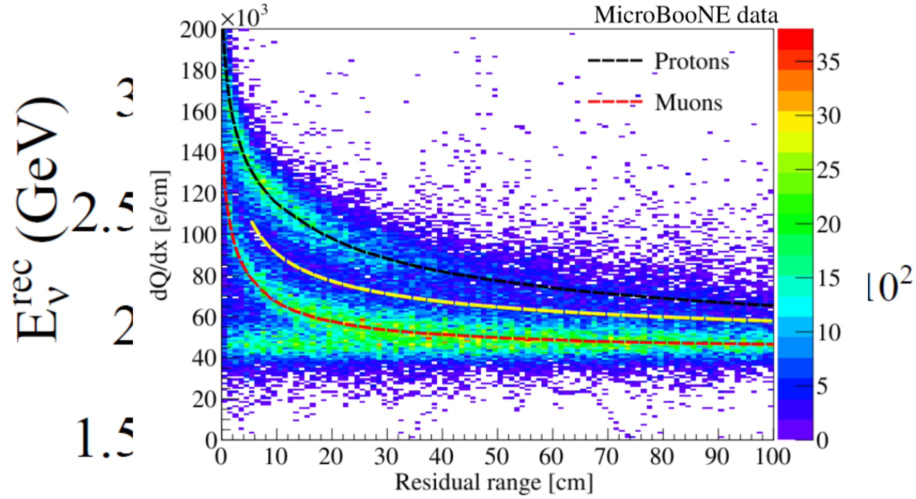

- Calorimetry energy reconstruction with particle mass and binding energy included if PID can be done
  - Track: Range, dQ/dx → dE/dx correction
    - Calibrated by stopped muons/protons
  - EM shower: scaling of charge
    - Calibrated by π^0 invariance mass

- Fully contained events

$\nu_e CC$ 10-15% resolution ~7% bia

$\nu_\mu CC$ 15-20% resolution ~10% bias

[arXiv:2110.13961](https://arxiv.org/abs/2110.13961)

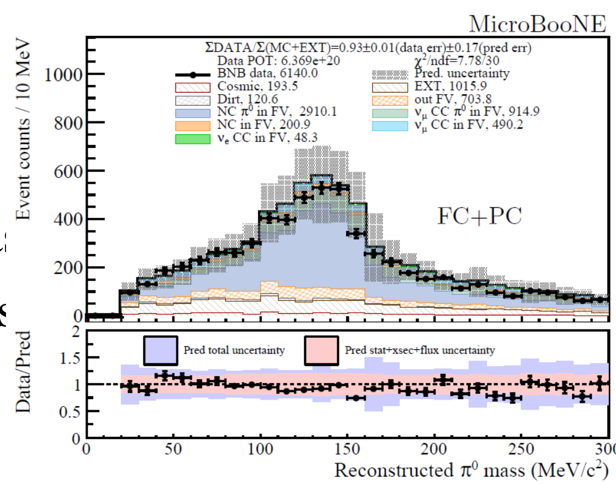

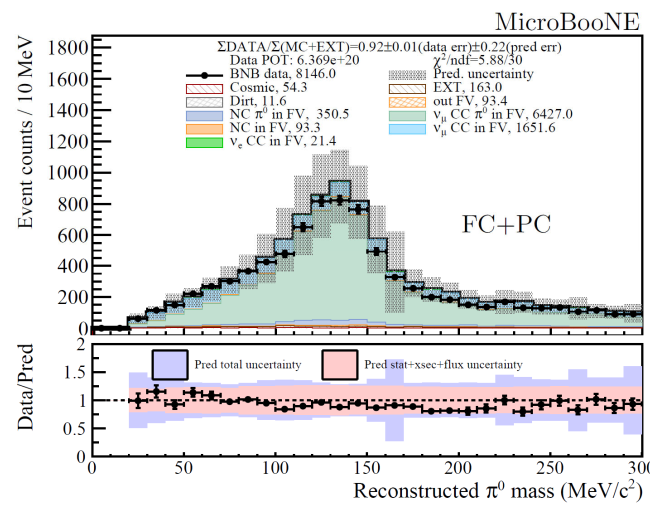

Neutrino Selection through Machine Learning

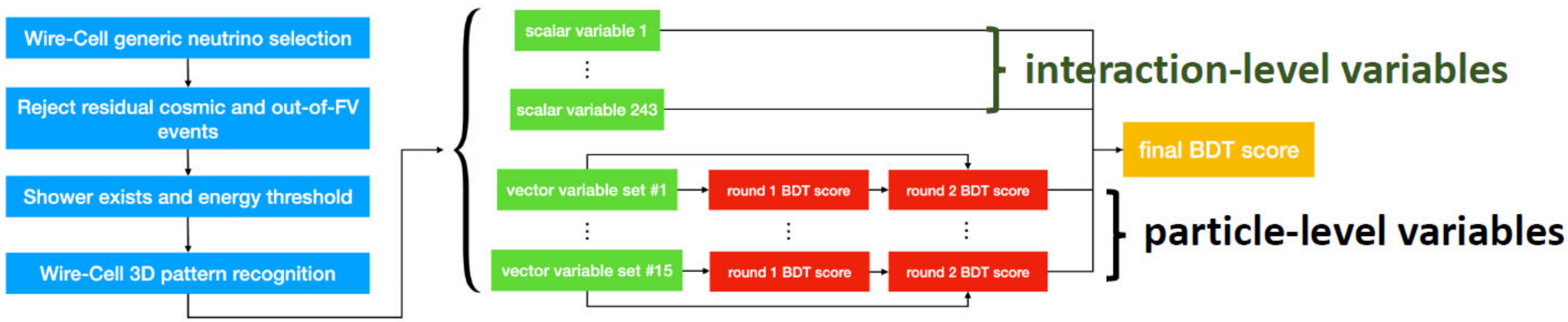

Human feature engineering

+

Maching learning algorithm:
XGBOOST: extreme Gradient Boosting

ν_μCC and ν_eCC Event Selection

arXiv:2110.13978

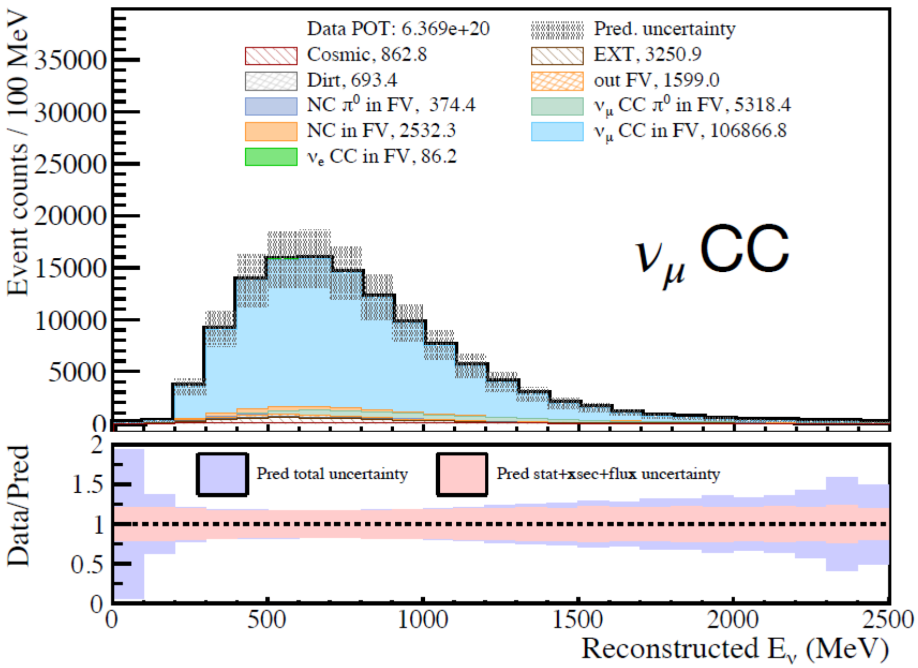

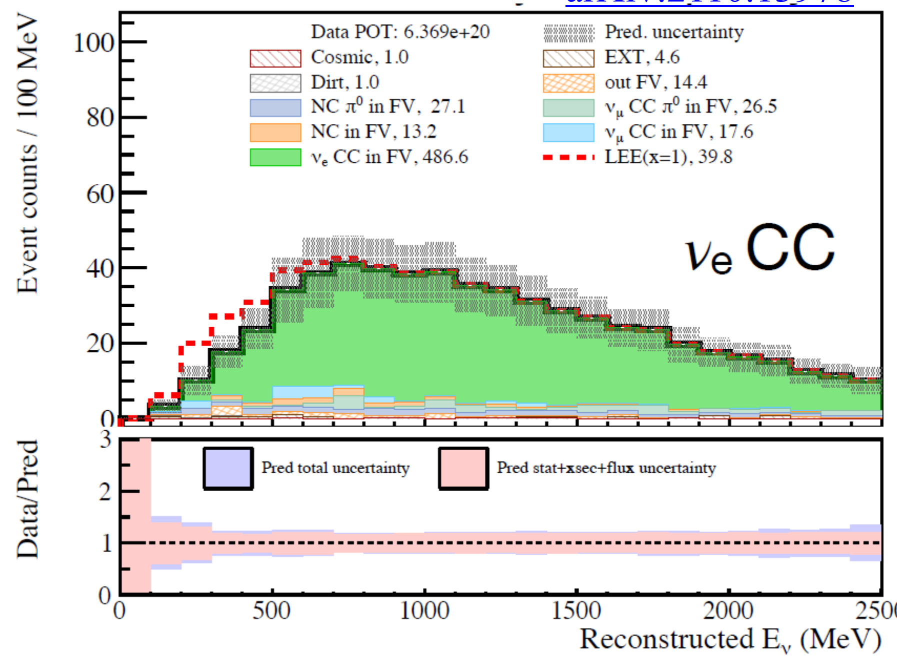

Efficiency: 68%
w.r.t to all ν_μCC w. vertex in fiducial volume
Purity: 92% (**>5** improvement in S/B)

Efficiency: 46%
w.r.t to all ν_eCC w. vertex in fiducial volume
Purity: 82% (**>800** improvement in S/B)

We are ready to do physics!

Application of Wire-Cell in Physics Analyses

Energy-dependent Cross Section

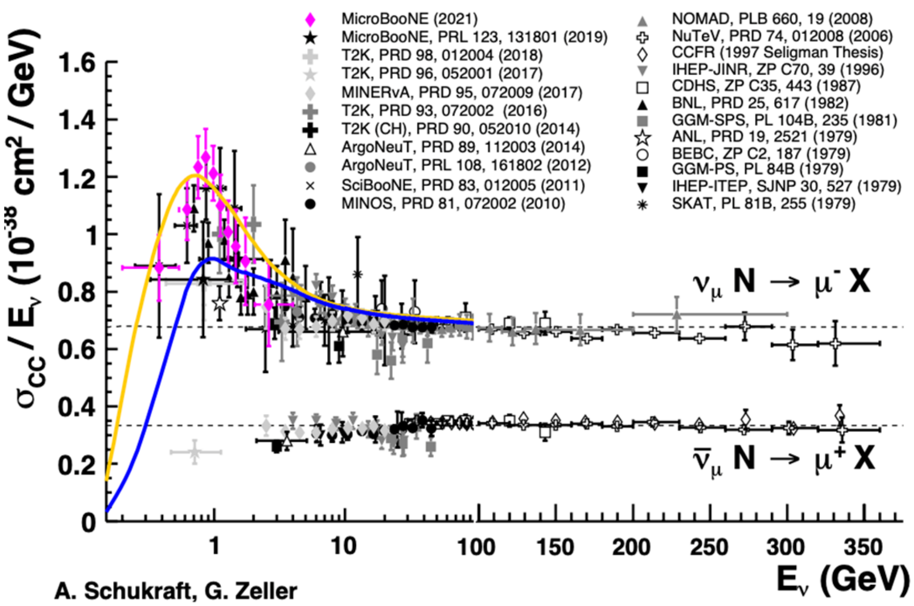

Search for ν_e Low Energy Excess

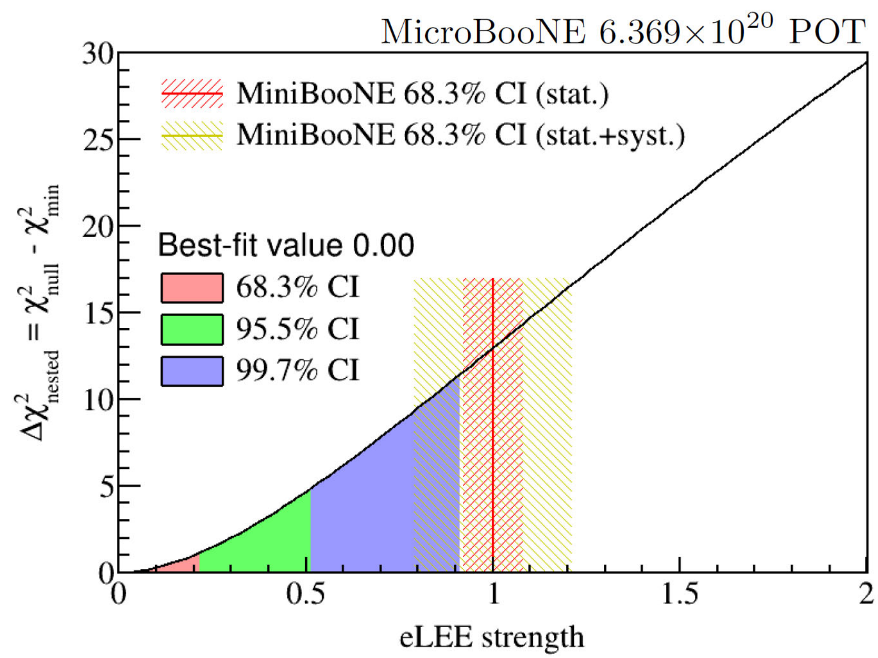

Systematic budget of Accelerator Neutrino Oscillation Measurements

- Cross section uncertainty is the dominant for accelerator oscillation experiments

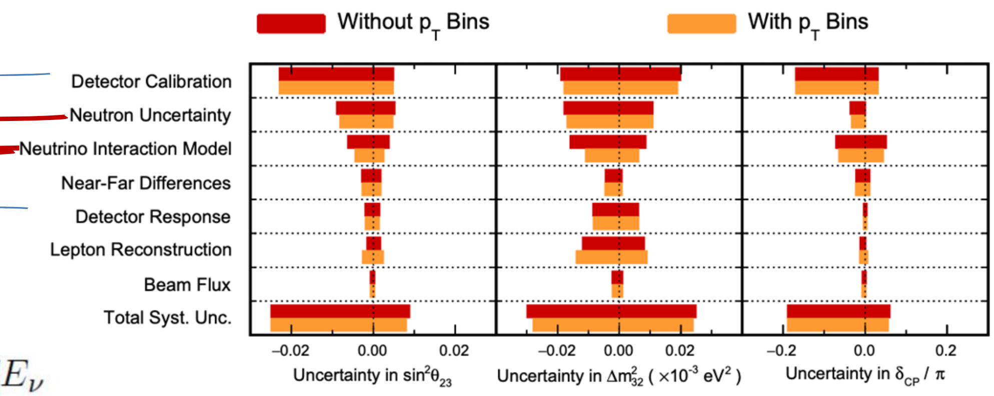

$$N^{far}(E_{reco}) = \int \Phi(E_\nu, L) \times \sigma(E_\nu) \times \epsilon(E_\nu) \times \mathbf{D}(E_\nu \rightarrow E_{reco}) dE_\nu$$

$$N^{near}(E_{reco}) = \int \Phi(E_\nu, 0) \times \sigma(E_\nu) \times \epsilon(E_\nu) \times \mathbf{D}(E_\nu \rightarrow E_{reco}) dE_\nu$$

QRyD du[ly=543;13;54<#
+vlp ldu#g#W5N,

- It's important to understand
  - Energy dependence of the inclusive cross section: $\boldsymbol{\sigma(E_\nu)}$
  - Mapping: $\mathbf{D}(\boldsymbol{E_\nu} \rightarrow \boldsymbol{E_{reco}})$

Evolved cross section extraction method

- Forward-folding

$$\left(\frac{d\sigma}{dp_\mu}\right)_i = \frac{N_i - B_i}{\tilde{\epsilon}_i \cdot N_{\text{target}} \cdot \Phi_{\nu_\mu} \cdot (\Delta p_\mu)_i}$$

N_i (B_i): # of candidate (bkgd) in reco bin i
N_{target} : # of argon nuclei
Φ_{ν_μ}: integrated neutrino flux
$(\Delta p_\mu)_i$: width for reco bin i
$\tilde{\epsilon}_i$: effective efficiency for reco bin i

- (Wiener-SVD) unfolding

$$\boldsymbol{N_i = \sum_j R_{ij} \cdot S_j + B_i}$$

N_i (B_i): # of candidate (bkgd) in reco bin i
R_{ij}: response (smearing) matrix
S_j: cross section to be extracted in **true bin j**

➥ Flux shape uncertainty properly treated ‡

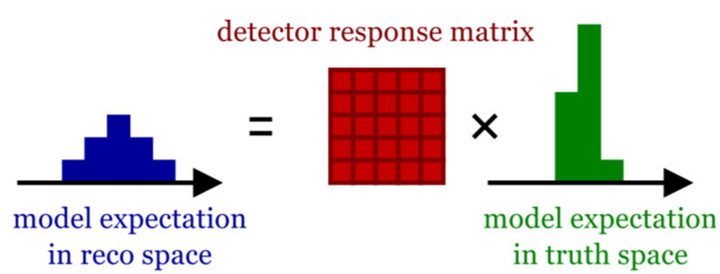

Wiener-SVD: JINST 12 (2017) 10, P10002

‡ : Phys. Rev. D 102 (2020) 113012

Evolved inclusive ν_μCC measurement

- Enhanced event selection efficiency **(57%→68%) and purity (50%→92%)**
- Extracted neutrino energy-dependent inclusive ν_μCC cross section
- **Challenge**: how to verify the modeling of the undetected **missing hadronic energy**?
  - ➥ Mapping of $E_\nu \rightarrow E_\nu^{rec}$

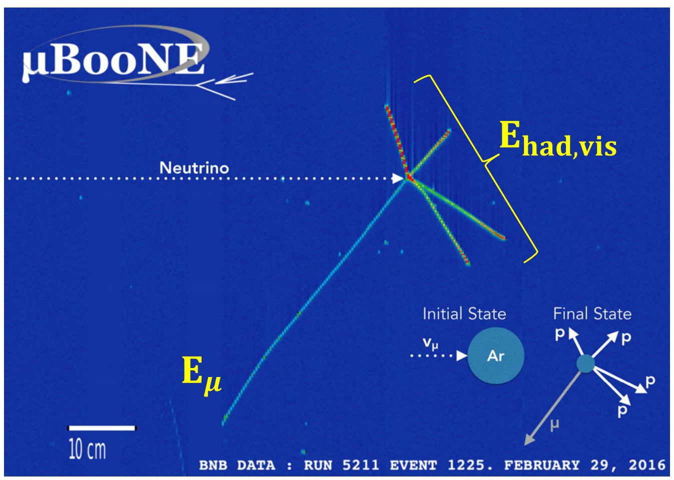

True energy components:

$$E_\nu = E_\mu + E_{had,vis} + E_{had,missing}$$

Calorimetric energy reconstruction:

$$E_\nu^{rec} = E_\mu^{rec} + E_{had,vis}^{rec}$$

Conditional constraining procedure

- Overcome the challenge by leveraging LArTPC's simultaneous measurements of **lepton energy** and **visible hadronic energy**

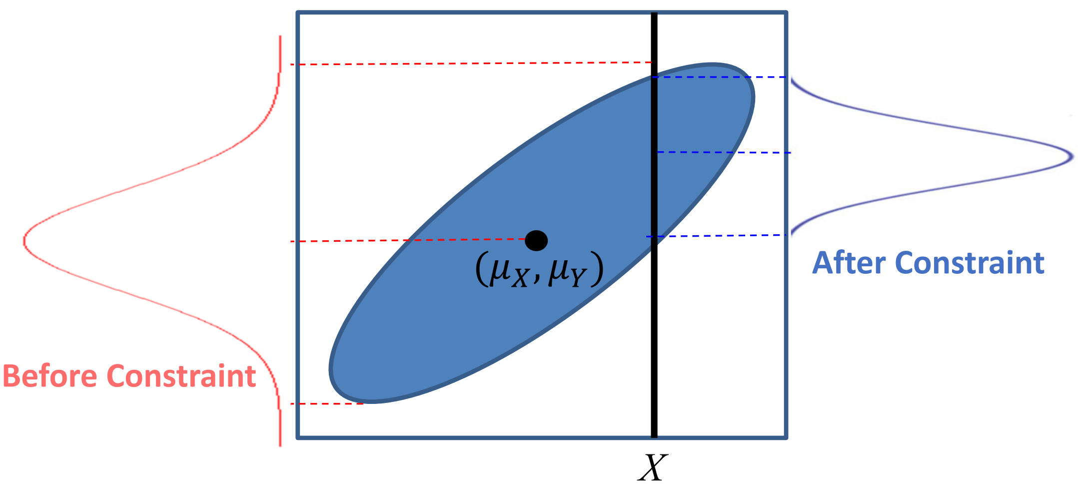

* Estimate correlated statistical uncertainty with bootstrapping (sampling w/ replacement)

Conditional expectation & covariance

$$\mu_{X,Y} = \begin{pmatrix} \mu_X \\ \mu_Y \end{pmatrix}, \qquad \Sigma_{X,Y} = \begin{pmatrix} \Sigma_{XX} & \Sigma_{XY} \\ \Sigma_{YX} & \Sigma_{YY} \end{pmatrix}$$

$$\mu_{Y|X} = \mu_Y + \Sigma_{YX}\Sigma_{XX}^{-1}(X - \mu_X)$$

$$\Sigma_{Y|X} = \Sigma_{YY} - \Sigma_{YX}\Sigma_{XX}^{-1}\Sigma_{XY}$$

* A variant of Gaussian Process regression

$$\begin{matrix} \mu(E_{had}^{rec}) \\ \Sigma(E_{had}^{rec}) \end{matrix} + M(E_\mu^{rec}) = \begin{matrix} \mu(E_{had}^{rec} \mid E_\mu^{rec}, E_\nu) \\ \Sigma(E_{had}^{rec} \mid E_\mu^{rec}, E_\nu) \end{matrix}$$

Prior model | Sideband | Posterior model

$$E_\nu = E_\mu + E_{had,vis} + E_{had,missing}$$

Model Validation: M($\mathbf{E}_{\text{had}}^{\text{rec}}$) vs. $\mu(\mathbf{E}_{\text{had}}^{\text{rec}} \mid \mathbf{E}_{\nu}, \mathbf{E}_{\mu}^{\text{rec}})$

Neutrino flux modeling

Measurement of muon kinematics

- New method to <u>validate modeling of neutrino energy</u> reconstruction given separated lepton and hadronic energy measurements in LArTPC

$$\mathbf{E}_{\nu} = \mathbf{E}_{\mu} + \mathbf{E}_{\text{had,vis}} + \mathbf{E}_{\text{had,missing}}$$

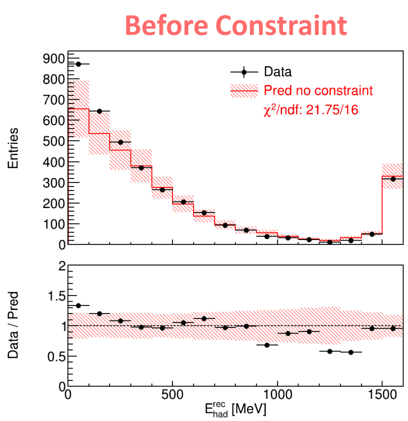

Excess at low hadronic energy indicates mis-modeling of missing energy?

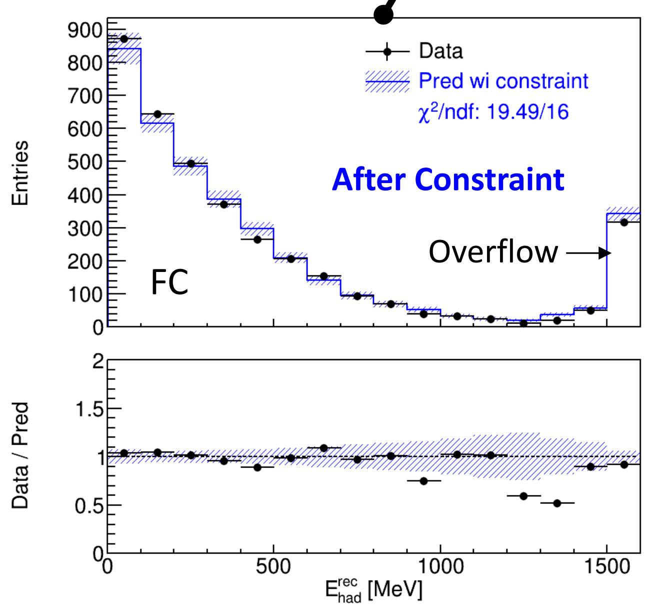

Measured muon kinematics are used to constrain the overall model (flux, cross section, etc.) for hadronic energy

- Systematic uncertainties 20% → 5% in performing model validation
- No more excess at low hadronic energy with constraints from muon
- No sign of mis-modeling of the **missing hadronic energy**

Cross-section results and model comparison

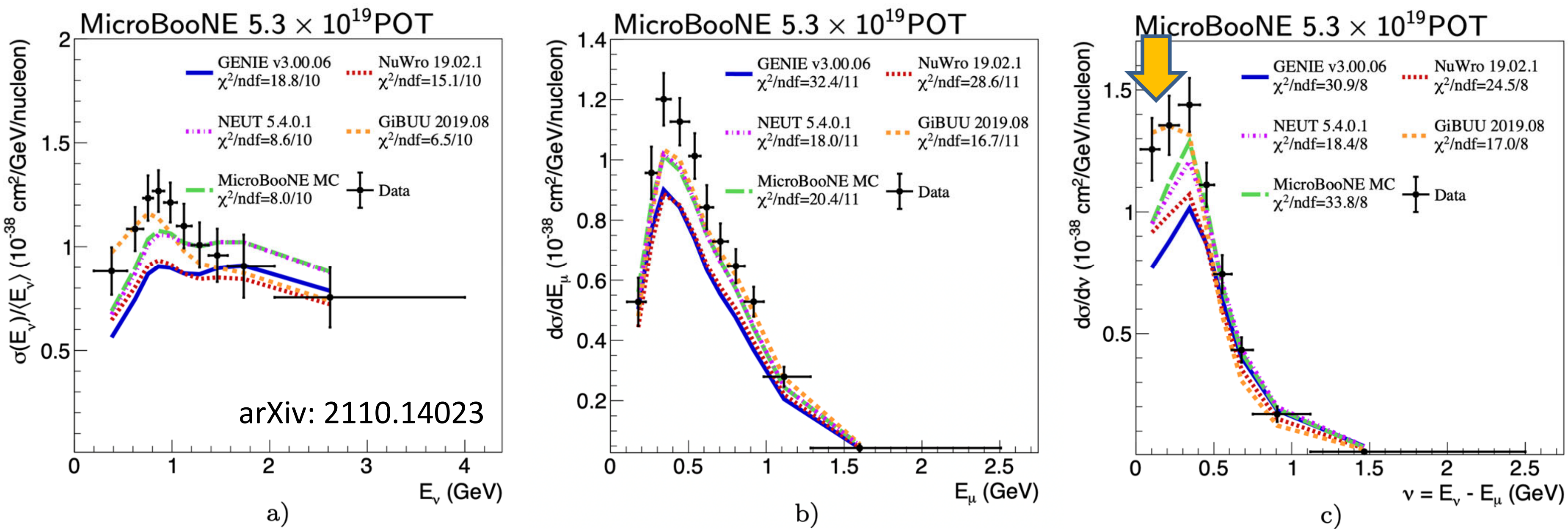

- Good separation power of model predictions from different generators
- GiBUU's central prediction gives best agreement at low energy transfer for Ar ⇒ more contribution of 2p2h

Model of eLEE for the Search in MicroBooNE

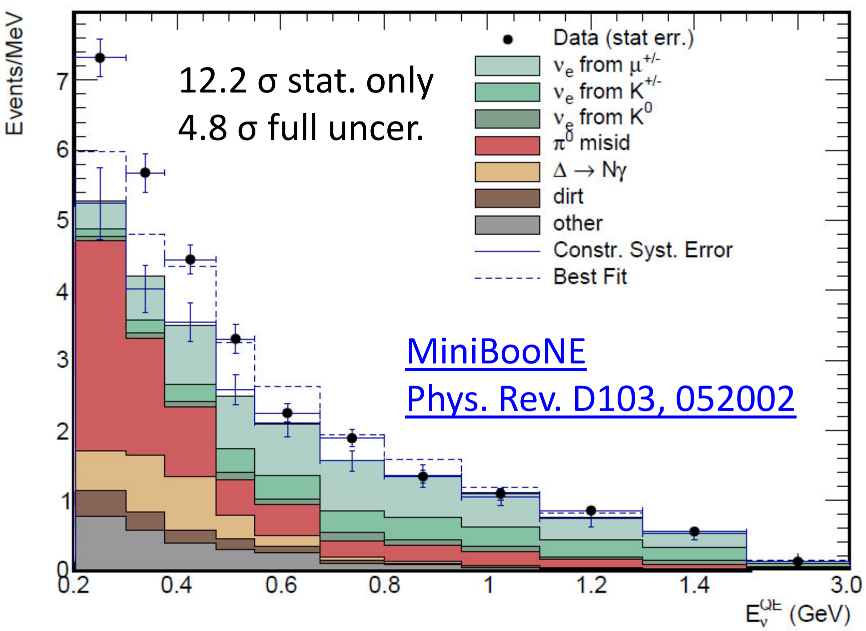

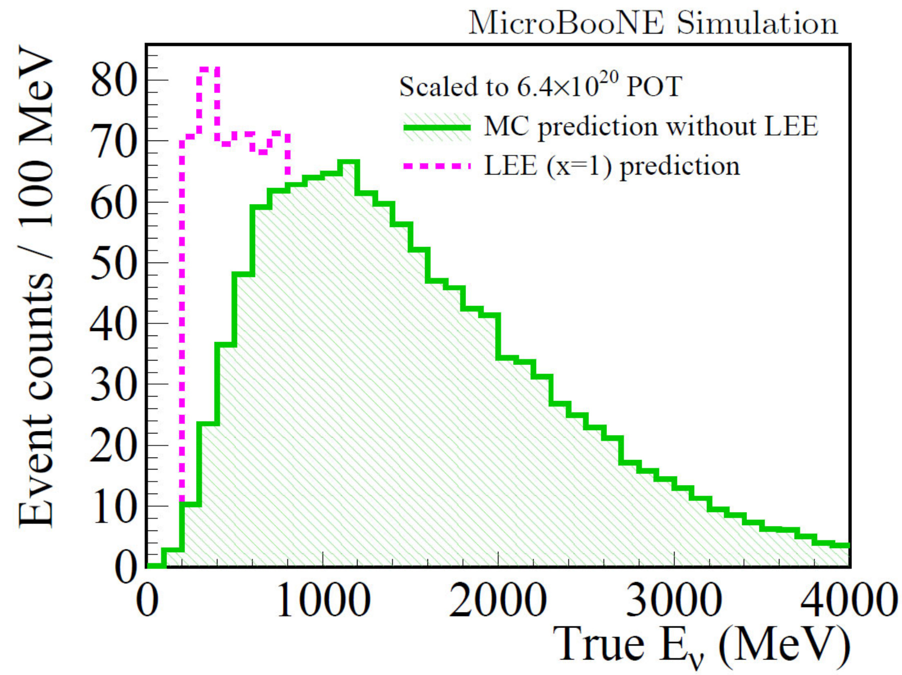

- eLEE is built upon the intrinsic ν_e as a function of neutrino energy
  - Unfolded from MiniBooNE observation and applied to MicroBooNE
- One normalization parameter 'x' built in the model

$$\text{MiniBooNE } x = \begin{cases} 1 \pm 0.08 \text{ (stat.)} \\ 1 \pm 0.21 \text{ (full)} \end{cases}$$

General Analysis Strategy

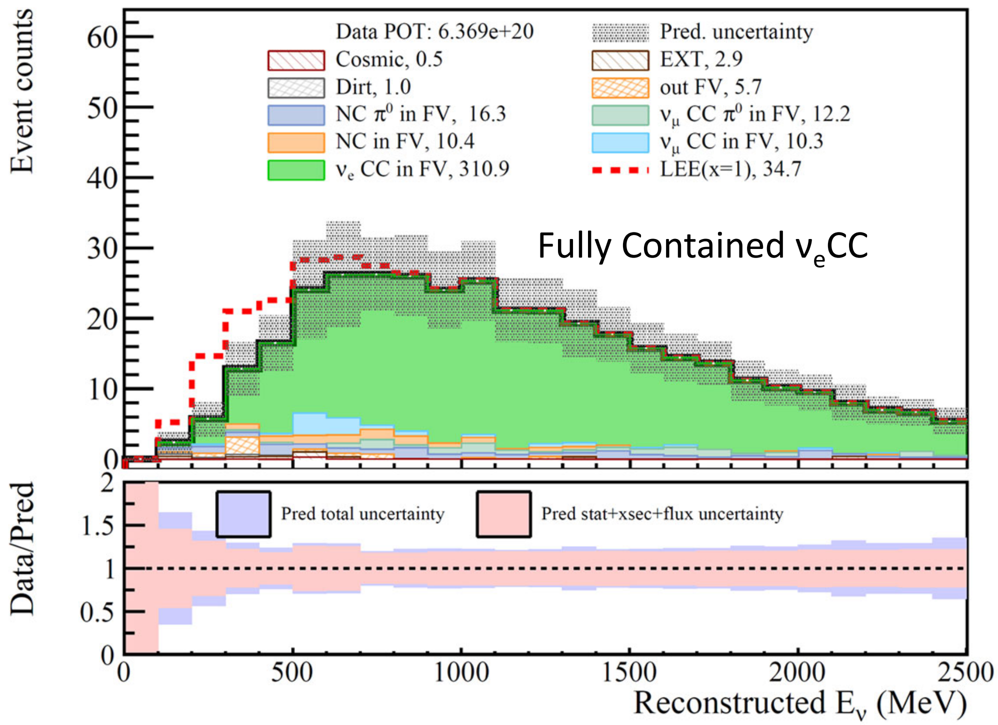

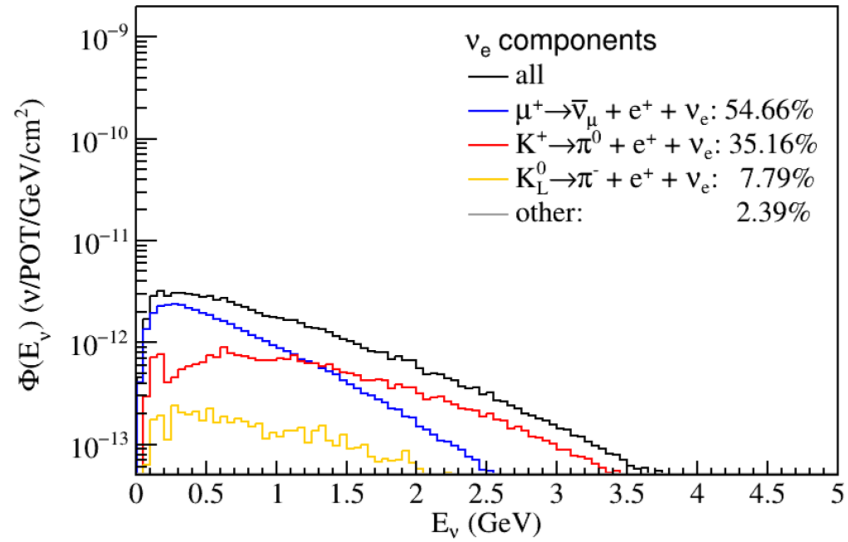

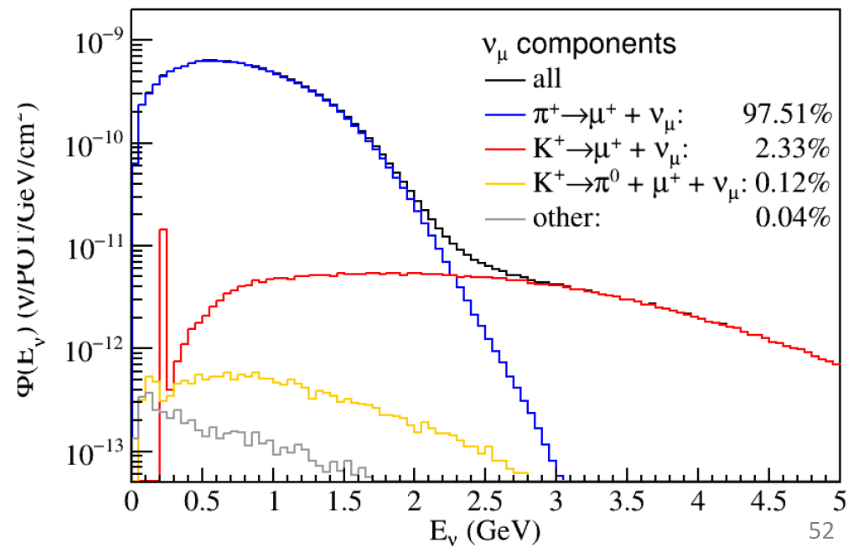

Seven-channel fit

Signal Constraints

ν_μCC Full Contained

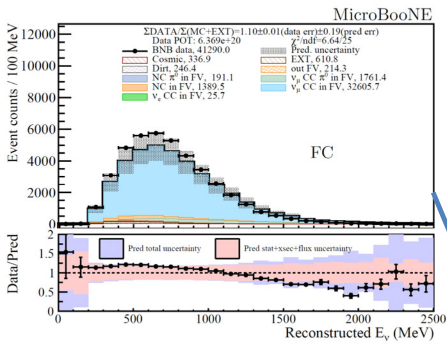

ν_μCC Partially Contained

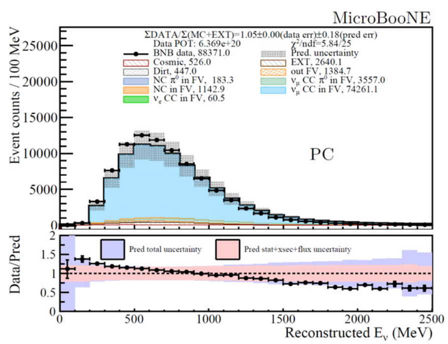

ν_eCC Partially Contained

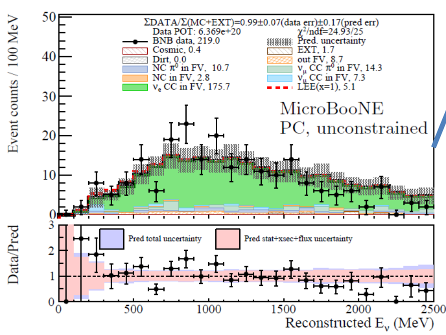

Reco neutrino energy

ν_e CC Fully Contained

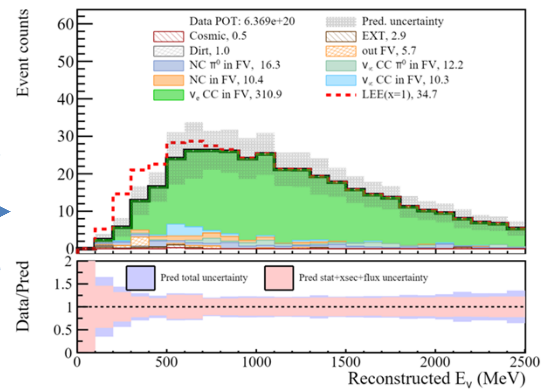

Reco neutrino energy

Background Constraints

CCπ^0 Fully Contained

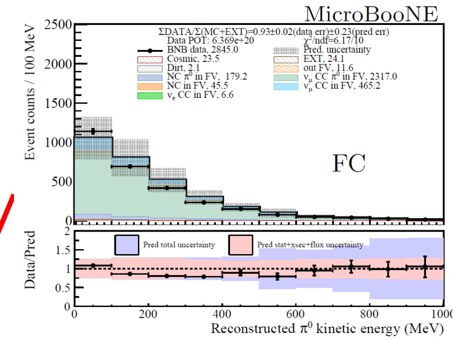

CCπ^0 partially Contained

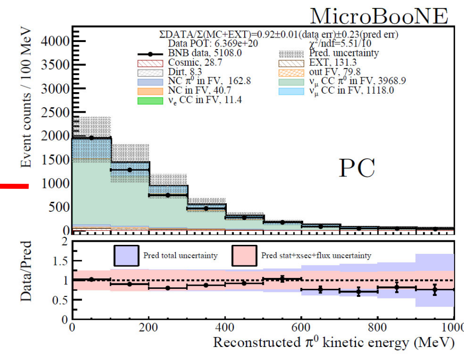

NCπ^0

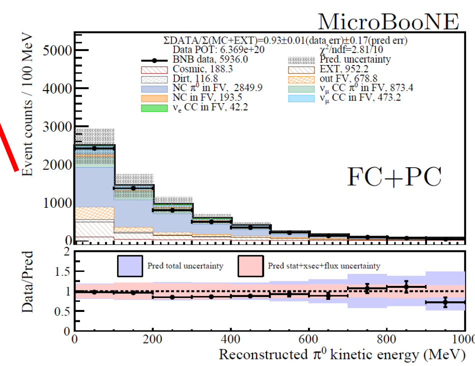

Reco. pi0 energy

Impact of Signal and Background Constraints

Before

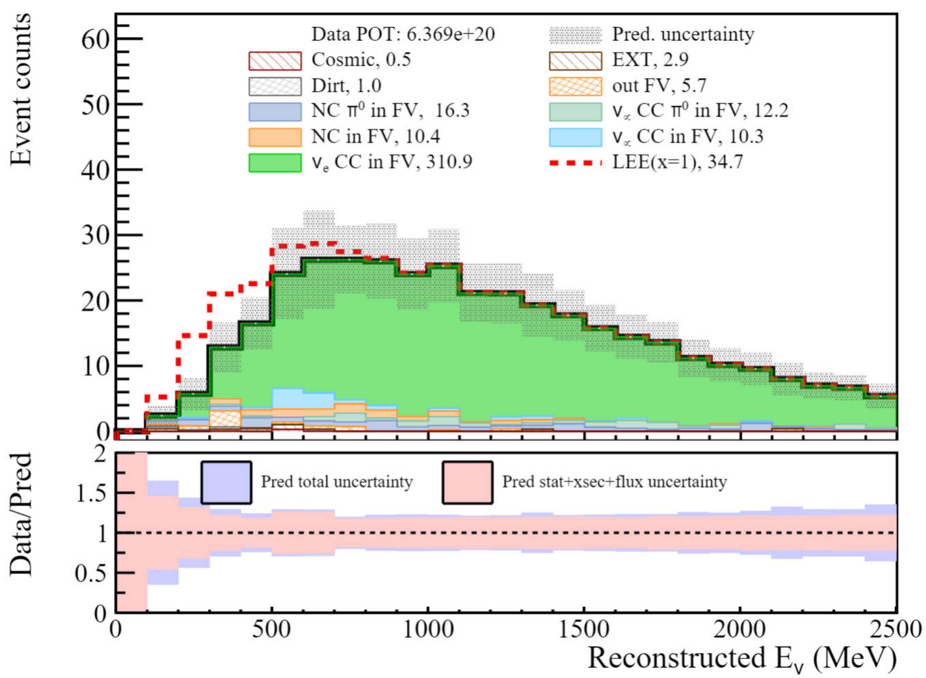

systematics reduced by more than a factor of 3

After Constraints and Unblinding

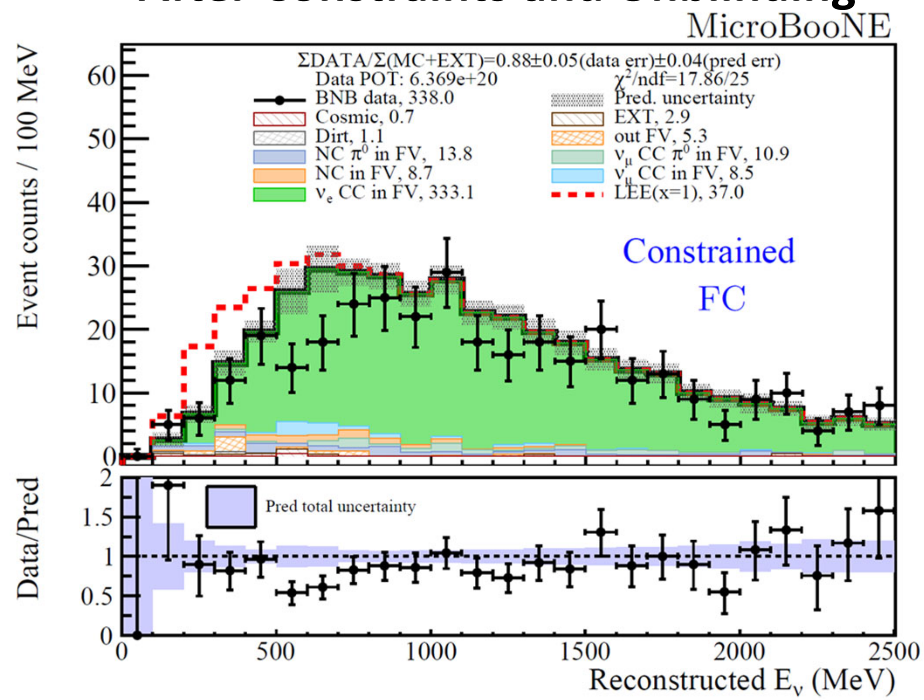

No excess of low-energy ν_e candidates!

Nested Hypothesis Test with free floating LEE strength

- Best-fit LEE strength at zero, given a slight deficit is observed in the signal region

- 68% stat-only uncer. MiniBooNE CI is disfavored at over 3σ
- 68% full uncer. MiniBooNE CI is disfavored at over 2.6σ

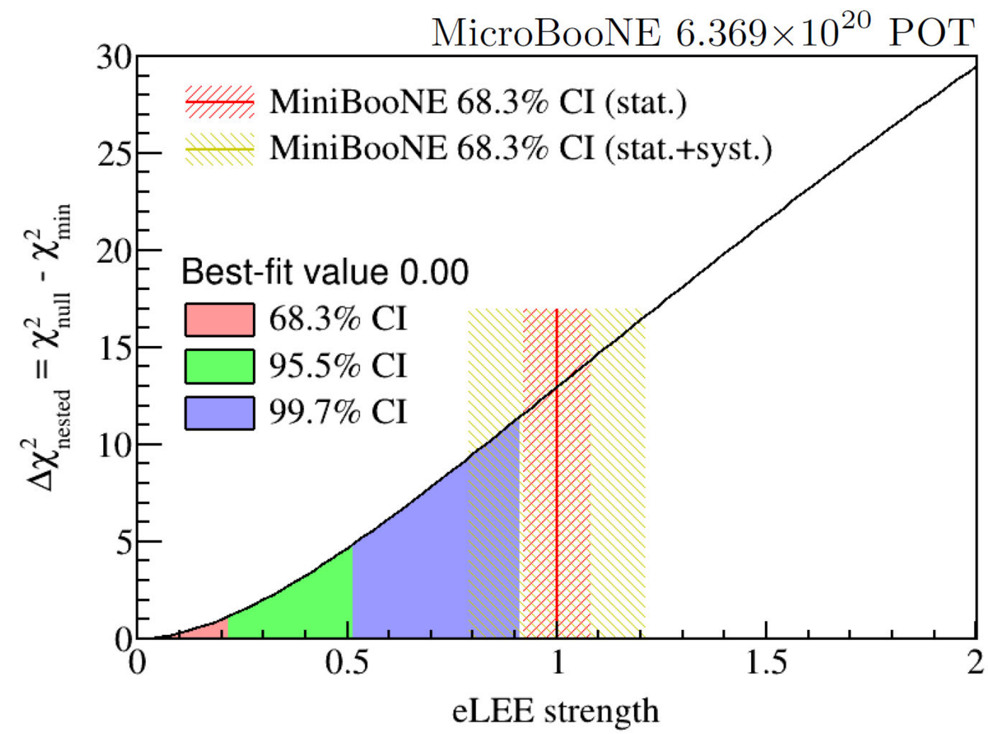

arXiv:2110.13978

ν_e cannot be the sole explanation of MiniBooNE LEE!

Search for Low-Energy Excess in ν_eCC

- Comprehensive search for (examination of) the MiniBooNE low-energy excess in ν_eCC with multiple final-state topologies with different reconstruction paradigms

Channels	Reconstruction	Purity	Data Events	References
CCQE 1e1p	Deep Learning	75%	25	2110.14080
1e0p0π	Pandora	43%	34	2110.14065
1eNp0π	Pandora	80%	64	2110.14065
Inclusive 1eX	**Wire-Cell**	82%	606	2110.13978

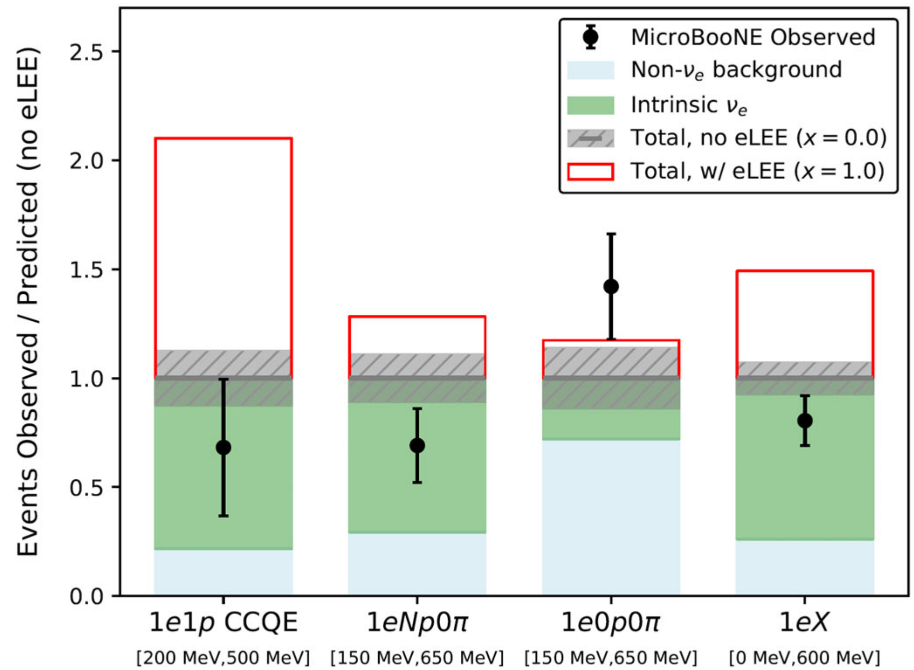

Wire-Cell based inclusive ν_eCC analysis (46% efficiency) currently leads sensitivity in searching for the LEE

arXiv:2110.14054

No excess of low-energy ν_e candidates!

Summary (I): Wire-Cell Event Reconstruction Chain

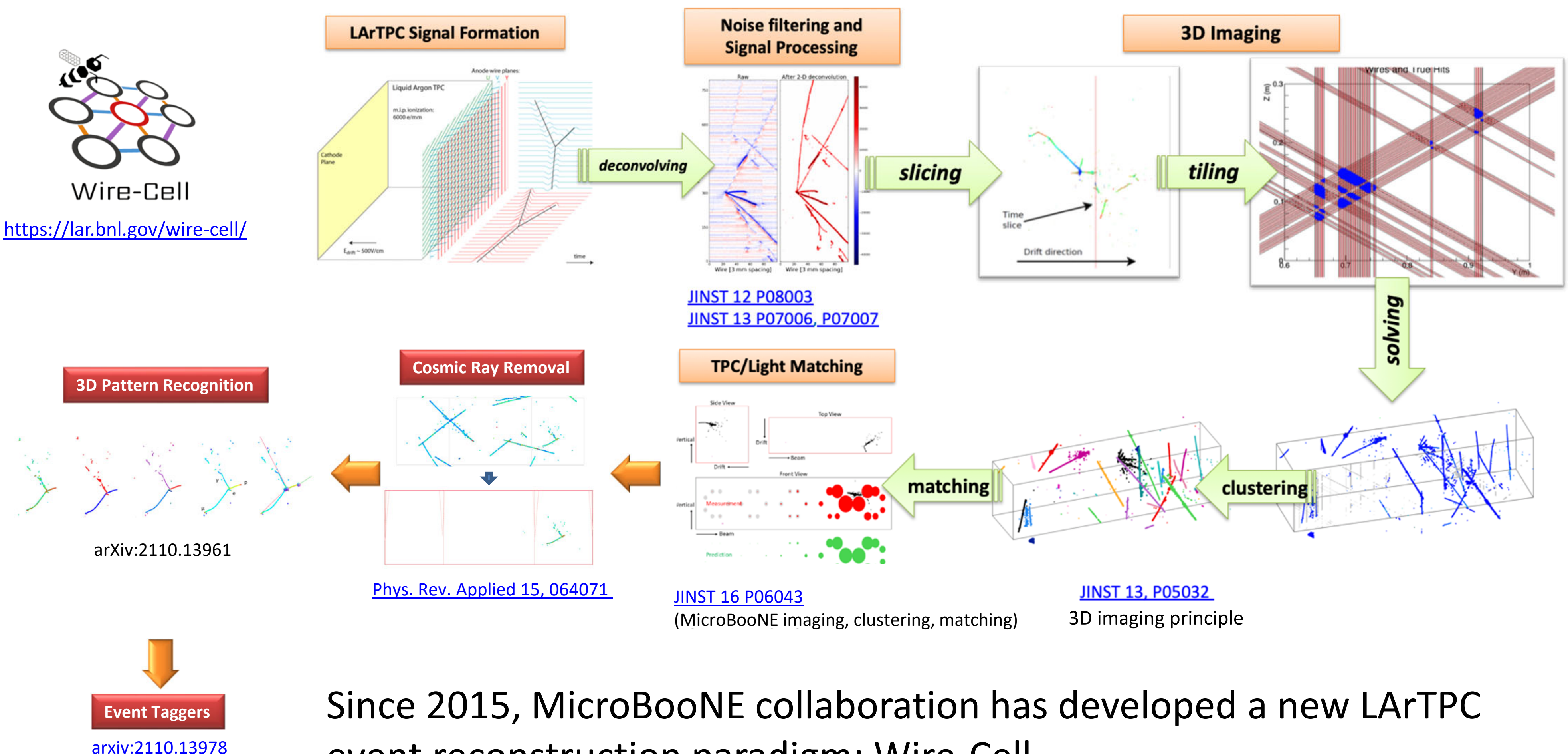

Since 2015, MicroBooNE collaboration has developed a new LArTPC event reconstruction paradigm: Wire-Cell

Summary (II)

- The development of Wire-Cell has paid off in the MicroBooNE experiment

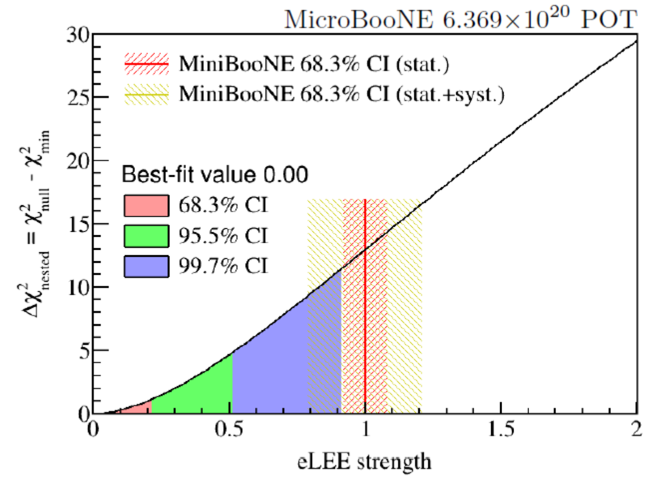

- The LArTPC technology advancements made by MicroBooNE is building a solid foundation for next discoveries in neutrino physics (SBN & DUNE)

MicroBooNE

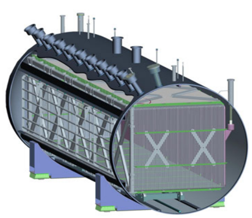

SBND

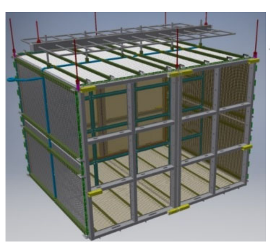

ProtoDUNE SP

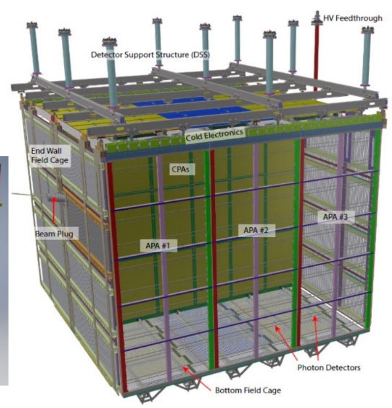

DUNE FD, SP

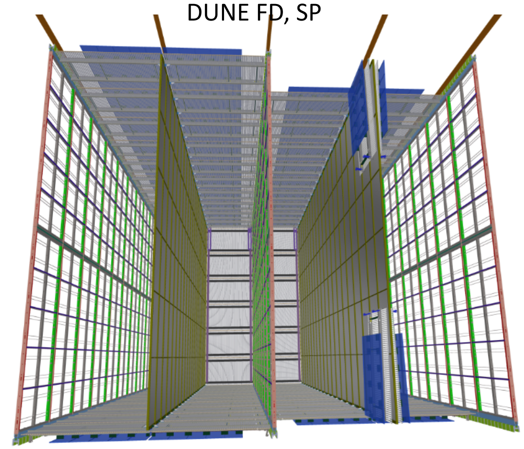

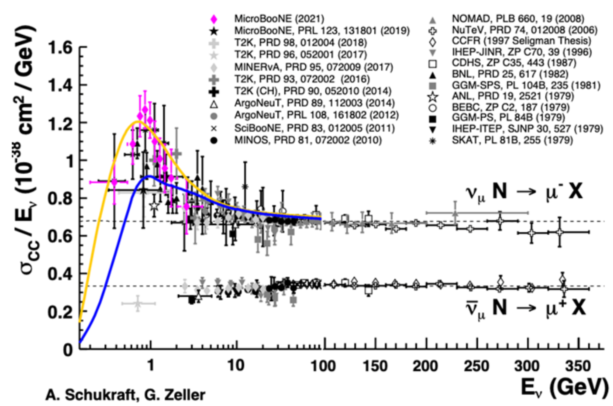

$\sigma(E_\nu)$